3-1-2017

Nitric oxide promotes GABA release by activating a voltage-independent Ca^{2+} influx pathway in retinal amacrine cells

J. Wesley Maddox
Louisiana State University

Evanna Gleason
Louisiana State University

Recommended Citation

Maddox, J., & Gleason, E. (2017). Nitric oxide promotes GABA release by activating a voltage-independent Ca^{2+} influx pathway in retinal amacrine cells. *Journal of Neurophysiology, 117* (3), 1185-1199. https://doi.org/10.1152/jn.00803.2016

J Neurophysiol 117: 1185–1199, 2017.
First published January 4, 2017; doi:10.1152/jn.00803.2016.

RESEARCH ARTICLE | *Cellular and Molecular Properties of Neurons*

Nitric oxide promotes GABA release by activating a voltage-independent Ca^{2+} influx pathway in retinal amacrine cells

J. Wesley Maddox and Evanna Gleason
Department of Biological Sciences, Louisiana State University, Baton Rouge, Louisiana

Submitted 11 October 2016; accepted in final form 30 December 2016

Maddox JW, Gleason E. Nitric oxide promotes GABA release by activating a voltage-independent Ca^{2+} influx pathway in retinal amacrine cells. *J Neurophysiol* 117: 1185–1199, 2017. First published January 4, 2017; doi:10.1152/jn.00803.2016.—Retinal amacrine cells express nitric oxide (NO) synthase and produce NO, making NO available to regulate the function of amacrine cells. Here we test the hypothesis that NO can alter the GABAergic synaptic output of amacrine cells. We investigate this using whole cell voltage clamp recordings and Ca^{2+} imaging of cultured chick retinal amacrine cells. When recording from amacrine cells receiving synaptic input from other amacrine cells, we find that NO increases GABAergic spontaneous postsynaptic current (sPSC) frequency. This increase in sPSC frequency does not require the canonical NO receptor, soluble guanylate cyclase, or presynaptic action potentials. However, removal of extracellular Ca^{2+} and buffering of cytosolic Ca^{2+} both inhibit the response to NO. In Ca^{2+} imaging experiments, we confirm that NO increases cytosolic Ca^{2+} in amacrine cell processes by activating a Ca^{2+} influx pathway. Neither the increase in sPSC frequency nor the cytosolic Ca^{2+} elevations are dependent upon Ca^{2+} release from stores. NO also enhances evoked GABAergic responses. Because voltage-gated Ca^{2+} channel function is not altered by NO, the increased evoked response is likely due to the combined effect of voltage-dependent Ca^{2+} influx adding to the NO-dependent, voltage-independent, Ca^{2+} influx. Insight into the identity of the Ca^{2+} influx pathway is provided by the transient receptor potential canonical (TRPC) channel inhibitor clemizole, which prevents the NO-dependent increase in sPSC frequency and cytosolic Ca^{2+} elevations. These data suggest that NO production in the inner retina will enhance Ca^{2+}-dependent GABA release from amacrine cells by activating TRPC channel(s).

NEW & NOTEWORTHY Our research provides evidence that nitric oxide (NO) promotes GABAergic output from retinal amacrine cells by activating a likely transient receptor potential canonical-mediated Ca^{2+} influx pathway. This NO-dependent mechanism promoting GABA release can be voltage independent, suggesting that, in the retina, local NO production can bypass the formal retinal circuitry and increase local inhibition.

nitric oxide; amacrine cells; synaptic transmission; GABA; Ca^{2+}

AMACRINE CELLS (ACs) are retinal interneurons that shape the visual signal in the inner retina via activity of their primarily glycinergic and GABAergic synapses. Most ACs have mixed-use dendrites because they are sites of both synaptic input and synaptic output. ACs form complex microcircuits by making reciprocal and serial inhibitory synapses with bipolar cells, ganglion cells and other ACs (Chávez et al. 2010; Grimes et al. 2010, 2015; Tsukamoto et al. 2001). These microcircuits are localized to AC dendrites, which can also have localized Ca^{2+} elevations (Euler et al. 2002).

Nitric oxide synthase (NOS) is a nitric oxide (NO) synthesizing enzyme that has two Ca^{2+}-sensitive isoforms: endothelial NOS (eNOS) and neuronal NOS (nNOS). Both of these enzymes have been localized to ACs as well as other retinal cell types (Fischer and Stell 1999; Haverkamp et al. 2000; Kim et al. 1999, 2000; Pang et al. 2010; Tekmen-Clark and Gleason 2013). nNOS has also been localized to AC presynaptic terminals in the inner turtle retina (Cao and Eldred 2001), suggesting that localized NO synthesis can affect neurotransmitter release.

The major signaling mechanisms for NO are through the cGMP pathway via activation of the canonical NO receptor, soluble guanylate cyclase (sGC), and through the direct chemical modification of proteins via *S*-nitrosylation. The light-dependent operation of both of these pathways appears to be widespread in the retina (Blom et al. 2012; Tooker and Vigh 2015). Although NO is typically viewed as diffusible, NO imaging has demonstrated that NO is largely confined to cellular boundaries in multiple retina cell types, including ACs (Eldred and Blute 2005; Tekmen-Clark and Gleason 2013). This implies that NO-dependent mechanisms can be localized to NO-producing cells and to their immediate synaptic partners.

The functions of NO in the retina are not fully known, but multiple sites of NO action have been identified. NO production is stimulated under photopic illumination and is known to be involved in light adaptation. For example, NO decouples horizontal cells (HCs) from other HCs (DeVries and Schwartz 1989; Miyachi et al. 1990) and decouples ON bipolar cells from A2 ACs (Mills and Massey 1995). NO can also affect the ON and OFF pathways. In retinal ganglion cells, NO reduces both ON and OFF light responses with the OFF responses being the most sensitive to NO (Wang et al. 2003). The mechanism underlying this inhibition of the pathway was not fully worked out, but the results pointed to an effect on neurons presynaptic to ganglion cells, most likely ACs. Thus AC synaptic function may be regulated by NO.

To test the hypothesis that NO can alter synaptic output from ACs, we employed whole cell current recordings and intracellular Ca^{2+} imaging in cultured chick ACs. We found that the

Address for reprint requests and other correspondence: E. L. Gleason, Dept. of Biological Sciences, Louisiana State University, Rm 202 Life Sciences Bldg., Baton Rouge, LA 70803 (e-mail: egleaso@lsu.edu).

NO donor *S*-nitroso-*N*-acetyl-DL-penicillamine (SNAP) increased both spontaneous and evoked GABAergic neurotransmission due to a NO-dependent increase of cytosolic Ca^{2+}. We find that a likely transient receptor potential canonical (TRPC)-mediated Ca^{2+} influx is required; however, Ca^{2+} release from stores is not. These data suggest that NO activates a presynaptic Ca^{2+} influx pathway that enhances GABAergic output from AC synapses in the retina.

METHODS

Amacrine cell cultures. The use of chick embryos to prepare retinal cultures was determined to be exempt by the Louisiana State University Institutional Animal Care and Use Committee. Eight-day white leghorn (*Gallus gallus*) chick embryo retinas were removed from the eyecup and dissected free of the retinal pigment epithelium. Retinas were initially dissociated in Ca^{2+}- and Mg^{2+}-free Hank's solution (Life Technologies, Grand Island, NY). The tissue was centrifuged (950 *g*), and the supernatant replaced with 0.125% trypsin (Sigma-Aldrich, St. Louis, MO). The pellet was resuspended and incubated at 37°C 5% CO_2 for 30 min. After incubation and centrifugation (1,900 *g*), the supernatant was replaced with Dulbecco's modified Eagle's medium (Life Technologies) supplemented with 5% fetal bovine serum (Sigma-Aldrich), penicillin (100 U/ml), streptomycin (100 μg/ml) and glutamine (2 mM) (Life Technologies). Cells were plated at a density of 2.5×10^5 cells/35-mm dish that were pretreated with 0.01% poly-DL-ornithine hydrobromide (Sigma Aldrich). Cultures were fed every other day after initial plating by replacing one-half of the media with neurobasal medium supplemented with 1% B-27, penicillin (100 U/ml), streptomycin (100 μg/ml) and glutamine (2 mM) (Life Technologies). Experiments were performed on ACs that had been in culture for 8–13 days (embryonic equivalent *days 16–21*). Over this time in culture, AC-to-AC GABAergic synapses are functional. ACs were identified on morphological criteria (Gleason et al. 1993).

Electrophysiology. Whole cell voltage clamp recordings were performed using Axopatch 1D amplifier, Digidata 1322A data-acquisition board, and Clampex 10.0 (Molecular Devices, Sunnyvale, CA). Patch pipette electrodes with a tip resistance between 5 and 10 MΩ for ruptured-patch recordings or 3–5 MΩ for perforated-patch recordings were pulled from thick-walled borosilicate glass (1.5 mm outer diameter, 0.86 mm inner diameter) using a P-97 Flaming/Brown Puller (Sutter Instruments, Novato, CA). A reference Ag/AgCl electrode pellet was placed in 3 M KCl and connected to the culture dish with a 3 M KCl agarose bridge. Recordings were performed at room temperature (22–24°C). A pressurized perfusion system (AutoMate Scientific, Berkeley, CA) was used to deliver external solutions at a flow rate of 1 ml/min. Most recordings were performed on postsynaptic ACs whose processes were in contact with unclamped presynaptic ACs and that had spontaneous postsynaptic currents (sPSCs). Variability of basal sPSC frequency depended on cell culture density. Denser cultures had higher basal sPSC frequency, possibly due to more synaptic sites. Cells that did not have basal sPSCs also did not respond to SNAP and were excluded from the analysis. Autaptic recordings were made from ACs that were not in contact with other ACs to eliminate the possibility that input was coming from unclamped cells.

Solutions. All reagents were purchased from Sigma-Aldrich, unless otherwise stated. Tetraethylammonium (TEA)-Cl external solution (in mM) contains the following (in mM): NaCl (117), KCl (5.3), TEA-Cl (20), $CaCl_2$ (3), $MgCl_2$ (0.41), glucose (5.6), HEPES (10), pH 7.4. LiCl (117 mM) replaced NaCl in evoked autaptic experiments to block the Na^+/Ca^{2+} exchanger current that can contaminate the autaptic currents at the end of the voltage step (see Fig. 8). Rupture-patch high Cl^- internal solution contains the following (in mM): CsCl (110), $MgCl_2$ (2), $CaCl_2$ (0.1), EGTA (1), HEPES (10), $NaCl_2$ (1), ATP-2Na^+ (3), ATP-2K^+ (1), GTP (2), phosphocreatine (20), creatine phosphokinase (50 U/ml), pH 7.4. Perforated-patch high Cl^- internal solution contains the following (in mM): CsCl (145), $MgCl_2$ (2), $CaCl_2$ (0.1), EGTA (1), HEPES (10), NaCl (1), pH 7.4, amphotericin B (200 μg/ml). Perforated-patch normal internal solution contains the following (in mM): Cs-acetate (135), $MgCl_2$ (2), $CaCl_2$ (0.1), EGTA (1), HEPES (10), NaCl (1), pH 7,4, amphotericin B (200 μg/ml). Typical reversal potential for Cl^- in cultured ACs is approximately −80 mV to −60 mV; however, these high Cl^- internal solutions increase the reversal potential of Cl^- to 0 mV, increasing the driving force on Cl^- and improving the resolution of quantal events. High internal Cl^- also blocks the NO-dependent release of Cl^- (Hoffpauir et al. 2006). While our laboratory has previously shown that the concentration of SNAP used here (500 μM) does not elicit Cl^- release (Hoffpauir et al. 2006), this internal further ensures that the NO-dependent release of Cl^- will not confound our results. For imaging experiments, the following external solutions were used: normal external solution containing (in mM) NaCl (137), KCl (5.37), $CaCl_2$ (3), $MgCl_2$ (0.41), glucose (5.6), HEPES (3.02), pH 7.4; and 0 Ca^{2+} external solution (0 Ca^{2+}_{ext}) containing (in mM) NaCl (141.5), KCl (5.37), $MgCl_2$ (0.41), glucose (5.6), HEPES (3.02), pH 7.4.

Reagents. The NO donor *S*-nitroso-*N*-acetyl-DL-penicillamine (SNAP, 500 μM; Enzo, Farmingdale, NY), the NO scavenger 2-[4-carboxyphenyl]-4,4,5,5-tetramethylimidazoline-1-oxyl-3-oxide (CPTIO, 10 μM, Enzo), bicuculline (10 μM), and tetrodotoxin (TTX; 300 nM; Abcam, Cambridge, MA) were dissolved directly into the external solution. 1,2-Bis(2-aminophenoxy)ethane-*N*,*N*,*N*′,*N*′-tetraacetic acid tetrakis (acetoxymethyl ester) (BAPTA-AM, 10 μM, Life Technologies) was prepared as a 10 mM stock in DMSO. The stock was diluted into Hank's balanced salt solution with $NaHCO_3$ (HBSS), briefly vortexed and sonicated for 30 s. Cells were incubated with BAPTA-AM at 37°C in 5% CO_2 for 45 min before recording. 1*H*-[1,2,4]oxadiazolo[4,3-*a*]quinoxalin-1-one (ODQ, 2 μM; Tocris, Bristol, UK), 2-aminoethoxydiphenylborane (2-APB, 20 μM; Tocris), 1-[2-(4-methoxyphenyl)-2-[3-(4-methoxyphenyl)propoxy]ethyl-1*H*-imidazole hydrochloride (SKF96365, 30 μM, Tocris), *N*-ethylmaleimide (NEM, 300 μM; Sigma), 1,4-dihydro-2,6-dimethyl-4-(2-nitrophenyl)-3,5-pyridinedicarboxylic acid dimethyl ester (nifidipine, 20 μM; Tocris), 6-cyano-7-nitroquinoxaline-2,3-dione (CNQX, 50 μM), and 1-[(4-chlorophenyl)methyl]-2-(1-pyrrolidinylmethyl)-1*H*-benzimidazole hydrochloride (clemizole, 10 μM; Tocris) were prepared as 1,000× stocks in DMSO and diluted to 1× in external solution. D-(-)-2-amino-5-phosphonopentanoic acid (D-AP5, 10 μM; Tocris) was prepared as a 10 mM stock and diluted in external solution. The sarco/endoplasmic reticulum Ca^{2+} ATPase (SERCA) pump inhibitor thapsigargin (TG; 2 μM; Enzo) was prepared as a 2 mM stock in DMSO and added directly to the culture media. Cells were incubated with TG at 37°C in 5% CO_2 for 1 h. The external solution pH was readjusted to 7.4 after the addition of reagents.

Calcium imaging. The fluorescent Ca^{2+} indicator Oregon Green 488 BAPTA-1, AM (OGB; 2 μM, Life Technologies) was prepared as a 2 mM stock in DMSO. OGB stock and Pluronic F-127 (2.5% wt/vol in DMSO, Life Technologies) were mixed in a 1:1 ratio and sonicated. Two microliters of the OGB/Pluronic mixture were diluted in 1 ml of HBSS and then briefly vortexed and sonicated for 30 s. Cells were incubated with the HBSS/OGB/Pluronic mixture for 1 h at room temperature (22–24°C). HBSS/OGB/Pluronic mixture was replaced with normal external solution. Images were taken every 500 ms (200-ms exposure, see Figs. 6, *A* and *B*, and 10, *C* and *D*), 3 s (400-ms exposure, see Fig. 4*A*), or 6 s (200-ms exposure, see Figs. 4*C* and 6, *E*, *F*, and *I*). To obtain data relevant to synaptic function, regions of interest (ROIs) were chosen at sites of contact between processes. Images were captured on an inverted Olympus IX70 microscope (Tokyo, Japan) fitted with a SensiCam QE (Cooke, Kelheim, Germany). Data were collected and analyzed using Slidebook software (Intelligent Imaging Innovations, Denver, CO). In all Ca^{2+} imaging experiments, the control fluorescence mean was calculated by using the average of the last 10 ROI time points before switching solutions,

and the fluorescence means after switching solutions were calculated by using the 10 ROI time points from the middle of each solution application. The control and different solution fluorescence means were used to calculate percent change in fluorescence.

Data analysis. For sPSC electrophysiology experiments, Mini Analysis Program (Synaptosoft, Fort Lee, NJ) was used to detect and analyze sPSCs. Quantal event kinetics were analyzed using data from Fig. 5, *A* and *C*, (No BAPTA) in which the recorded cells were only exposed to SNAP. Multiquantal events were removed from analysis by determining the mean and SD of the rise time of quantal events from control data where multiquantal events are extremely rare. Quanta with a rise time longer than 3.7 ms (mean rise time plus 1 SD) were excluded from the analysis. Mean amplitudes (pA), mean rise times (ms) and mean decay times (ms) were determined from each of the 9 recorded cells during control (254 total events) and application of SNAP (319 total events, 489 multiquantal events removed). Mean amplitude, mean rise time and mean decay time from each cell were used for statistical analysis. Charge transfer integration and Ca^{2+} current leak subtraction were performed using OriginPro (OriginLab, Northampton, MA). Charge transfer was calculated by integrating the area under the postdepolarization autaptic current waveform. The charge transfer integration (pA × s) was then calculated and reported as pC. After linear leak subtraction, activation voltage of voltage-gated Ca^{2+} channels (VGCCs) was measured at the point the Ca^{2+} current reached 5% of the maximum current amplitude. In autaptic and voltage-ramp experiments, perforated-patch configuration using amphotericin B (Sigma) was used to maintain the native presynaptic environment as much as possible during prolonged recording times. Because amphotericin B introduces an unknown liquid junction potential, voltages were left uncorrected. Statistics were performed using GraphPad Prisim 6 (GraphPad Software, La Jolla, CA). Repeated-measures ANOVA with Fisher's least significant difference post hoc analysis was performed on all data, unless otherwise indicated. Data are reported as means ± SE.

RESULTS

SNAP increases sPSC frequency. To determine whether NO affects spontaneous neurotransmitter release, ACs bearing processes in contact with other (unclamped) ACs were voltage clamped at −70 mV in TEA-Cl external solution. For sPSCs recordings, high-Cl^- internal solution was used to increase the driving force on Cl^- (at −70 mV). Under control conditions, sPSCs corresponding to quantal events were observed ranging in frequency from 1.4 to 77.6 events/30 s. When SNAP (500 μM) and the NO scavenger CPTIO (10 μM) were coapplied, no change in sPSC frequency was observed (control, 9.8 ± 3/30 s, SNAP/CPTIO, 10.7 ± 3/30 s, $P = 0.5$, $n = 8$, Fig. 1). When CPITO was removed and only SNAP was present, however, there was a 108% increase in sPSC frequency (SNAP/CPTIO, 10.7 ± 2.7/30 s, SNAP, 22.3 ± 5.2/30 s, $P = 0.03$, $n = 8$). NO did not affect the quantal event amplitude (control, 11.6 ± 0.8 pA, SNAP, 11.3 ± 1.2 pA, $P = 0.63$, $n = 9$ cells, paired *t*-test), rise time (control, 2.3 ± 0.1 ms, SNAP, 2.5 ± 0.1 ms, $P = 0.12$, $n = 9$ cells, paired *t*-test), or decay time (control, 9.55 ± 1.1 ms, SNAP, 9.9 ± 1.2 ms, $P = 0.86$, $n = 9$ cells, paired *t*-test). Thus these data indicate that NO, rather than the donor molecule or NO metabolites, increased presynaptic spontaneous vesicle fusion and neurotransmitter release but did not affect the postsynaptic receptors.

NO-dependent increase of sPSC frequency does not require sGC activity. The canonical receptor for NO is sGC. NO-activated sGC increases the production of the secondary messenger cGMP. To determine if NO-dependent activation of sGC and cGMP signaling was involved in the increase of sPSC frequency, cells were preincubated with the sGC inhibitor ODQ (2 μM) for 12 min before recording, and ODQ remained throughout the recording. Even in the presence of ODQ, SNAP caused a 173% increase in sPSC frequency (ODQ, 20.1 ± 4.5/30 s, ODQ/SNAP, 54.9 ± 15.0/30 s, $P = 0.03$, $n = 12$, Fig. 2). Acute application of ODQ alone did not alter sPSC frequency (control, 6.6 ± 3.19/30 s, ODQ, 5.25 ± 2.8/30 s, $P = 0.06$, $n = 4$, paired *t*-test). These data suggest that sGC does not mediate the NO-dependent increase in sPSC frequency.

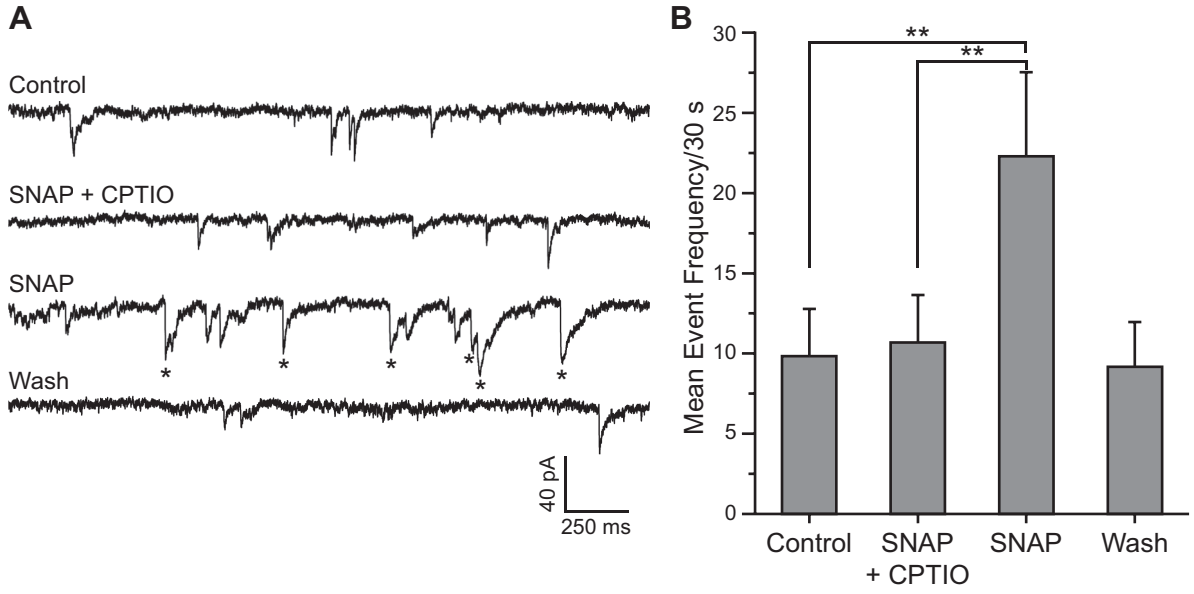

Fig. 1. NO increases frequency of spontaneous postsynaptic currents (sPSCs). *A*: recording from a representative postsynaptic AC voltage clamped at −70 mV and synaptically connected with other unclamped ACs. Coapplication of the NO donor SNAP (500 μM) and the NO scavenger CPTIO (10 μM) had no effect on the sPSC frequency. After removal of CPTIO, a significant increase sPSC frequency was observed. *Multiquantal events. *B*: quantified mean event frequency of sPSCs/30 s ± SE; $n = 8$. *$P < 0.05$, **$P < 0.01$ (repeated measures-ANOVA).

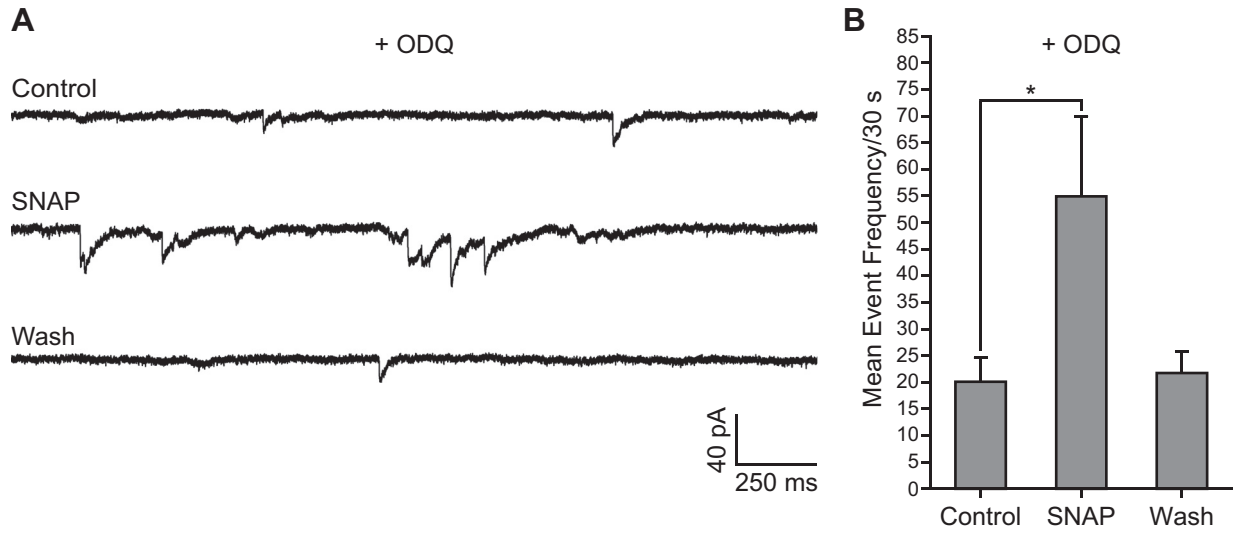

Fig. 2. NO-dependent increase of sPSCs does not require soluble guanylate cyclase (sGC) activity. *A*: recording from a representative AC held at −70 mV. Cells were exposed to the sGC inhibitor ODQ (2 μM) for at least 12 min before and throughout the recordings. SNAP increased the frequency of sPSCs in the presence of ODQ. *B*: quantified mean event frequency of sPSCs/30 s ± SE; $n = 12$. *$P < 0.05$ (paired *t*-test).

Because activation of the canonical NO receptor sGC is not required for the increase in sPSC frequency, we investigated the role of another NO signaling pathway, *S*-nitrosylation. *S*-nitrosylation occurs when NO reacts with a cysteine residue thiol group to form an *S*-nitrosothiol. *S*-nitrosylation posttranslational protein modification is similar to phosphorylation in that it can alter the function of the targeted protein. NEM, a known inhibitor of *S*-nitrosylation, was used to investigate if *S*-nitrosylation was involved in the NO-dependent increase in sPSC frequency. NEM (300 μM), however, caused an increase in sPSC frequency from baseline by 411% (control, 24.2 ± 15.26/30 s, NEM, 123.5 ± 26.78/30 s, $P = 0.007$, $n = 7$, paired *t*-test). Unfortunately, NEM has multiple targets, including presynaptic proteins (Clary et al. 1990; Peters et al. 1990; Rothman 1996) and has been shown to increase GABAergic spontaneous neurotransmitter release (Kirmse and Kirischuk 2006; Knight et al. 2004) and activate some Ca^{2+} channels (Bindoli and Fleischer 1983; Graham et al. 2010; Pan et al. 2011). These results precluded further experiments using NEM in this study.

NO increases GABAergic sPSC frequency. ACs in these cultures have been demonstrated to be GABAergic (Gleason et al. 1993). However, to confirm that NO is promoting the release of GABA rather than an additional neurotransmitter, the ionotropic GABA receptor antagonist bicuculline (10 μM) was added to the extracellular solution during the application of SNAP. SNAP caused a 190% increase in sPSC frequency (control, 7.6 ± 2.0/30 s to SNAP, 22.1 ± 5.7/30 s, $P = 0.02$; $n = 9$, Fig. 3, *A* and *B*). However, bicuculline caused a 99% reduction in NO-dependent sPSC frequency (SNAP, 22.1 ± 5.7/30 s, SNAP/bicuculline, 0.3 ± 0.1/30 s, $P = 0.003$, $n = 9$, Fig. 3, *A* and *B*). These data indicate that NO increased GABAergic sPSCs due to increased presynaptic vesicle fusion and GABA release, but not due to the release of any other neurotransmitter. Previous work from our laboratory demonstrated a small (~15%) NO-dependent enhancement of whole cell $GABA_A$ receptor currents, apparently due to an alteration in channel function (Hoffpauir et al. 2006). Here we see no effect of NO on sPSC current amplitude, suggesting that synaptic and extrasynaptic receptors may be differentially regulated.

NO-dependent increase of sPSC frequency is not action potential dependent. Some ACs are known to fire action potentials (APs) (Cook et al. 1998; Heflin and Cook 2007; Watanabe et al. 2003). For the experiments recording sPSCs (Figs. 1–3*A*), presynaptic ACs were unclamped, which allows their membrane potentials to fluctuate and possibly produce APs. To determine whether the NO-dependent increase of GABA release was due to presynaptic APs in response to NO, the voltage-gated Na^+ channel blocker TTX (300 nM) was included in the TEA-Cl external solution. In the presence of TTX, SNAP still elicited a 202% increase in sPSC frequency (TTX, 7.3 ± 2.0/30 s, TTX/SNAP, 22.1 ± 5.7/30 s, $P = 0.03$, $n = 5$, paired *t*-test, Fig. 3, *C* and *D*). This indicates that sPSC frequency was increased by a NO-dependent mechanism that does not require APs.

The role of Ca^{2+}. Vesicle fusion and neurotransmitter release depends on the local presynaptic Ca^{2+} concentration. To determine whether NO affects cytosolic Ca^{2+}, cytosolic Ca^{2+} levels were monitored using the fluorescent Ca^{2+} indicator OGB (2 μM). Data were collected from regions of neuronal process contacts, potentially synaptic sites. Coapplication of the NO scavenger CPTIO and SNAP did not significantly alter intracellular Ca^{2+} ($P = 0.17$, $n = 57$, Fig. 4, *A* and *B*). After removal of CPTIO, however, there was a 32% increase in intracellular Ca^{2+} [CPTIO/SNAP, 26.7 ± 1.2 arbitrary units (AU), SNAP, 35.3 ± 1.6 AU, $P < 0.0001$, $n = 57$, Fig. 4, *A* and *B*]. Additionally, there was an 11% reduction in cytosolic Ca^{2+} when external Ca^{2+} was removed during the SNAP application, (SNAP, 7.9 ± 0.5 AU, SNAP/0 Ca^{2+}, 7.0 ± 0.4 AU, $P < 0.0001$, $n = 35$, Fig. 4, *C* and *D*). These results indicated that NO, rather than the donor molecule or NO metabolites, increased intracellular Ca^{2+} via an extracellular Ca^{2+}-dependent mechanism.

Having established that NO can produce Ca^{2+} elevations in ACs, we asked whether the Ca^{2+} elevations were driving the NO-dependent increase in sPSCs. BAPTA-AM (10 μM), a cell-permeant fast Ca^{2+} chelator, was loaded into the cells

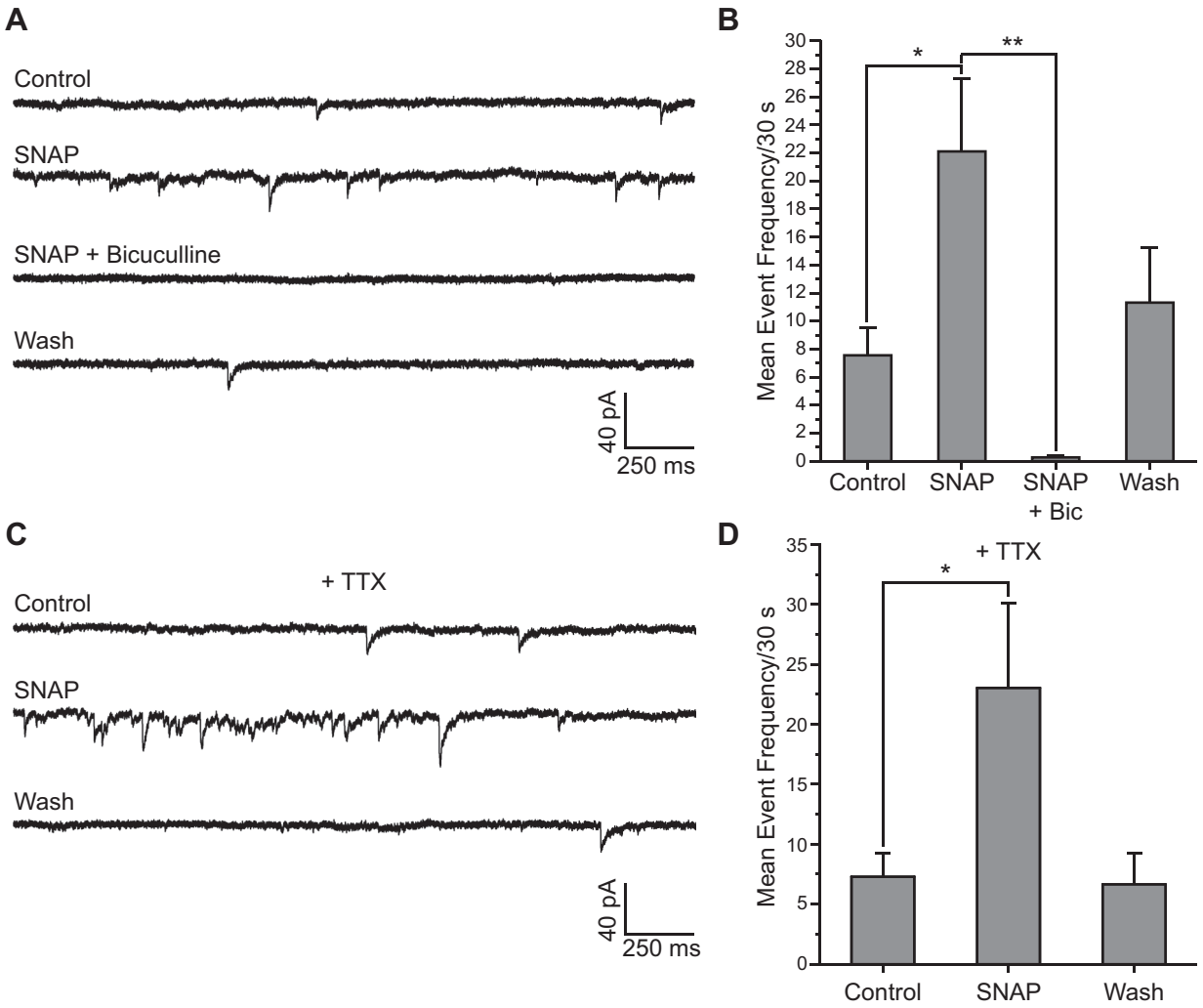

Fig. 3. NO-induced increase in GABAergic sPSC frequency does not require action potentials. *A*: recording from a representative postsynaptic AC held at −70 mV. Application of the NO donor SNAP increased the frequency of sPSCs. Addition of the $GABA_A$ receptor antagonist bicuculline abolished the NO-dependent increase of sPSCs, indicating that these are GABAergic sPSCs. *B*: quantified mean event frequency of sPSCs/30 s ± SE; $n = 9$. $^*P < 0.05$, $^{**}P < 0.01$ (repeated measures-ANOVA). *C*: voltage clamp recording from a representative postsynaptic AC held at −70 mV. SNAP increased the frequency of sPSCs in the presence of the voltage-gated Na^+ channel blocker TTX (300 nM). *D*: quantified mean event frequency of sPSCs/30 s ± SE; $n = 5$. $^*P < 0.05$ (paired *t*-test).

before recordings. In BAPTA-containing cells, sPSC frequency in the recorded cell was not enhanced by SNAP (control, 5.9 ± 1.1/30 s, SNAP, 6.4 ± 1.1/30 s, $P = 0.62$, $n = 12$, paired *t*-test, Fig. 5, *B* and *C*). In cells that did not have BAPTA, however, SNAP caused a 172% increase in sPSC frequency (control, 9.2 ± 1.3/30 s, SNAP, 25.0 ± 2.7/30 s, $P = 0.0002$, $n = 12$, paired *t*-test, Fig. 5, *A–C*). These results suggest that the NO-dependent increase in intracellular Ca^{2+} is responsible for the NO-dependent increase in sPSC frequency.

To determine if Ca^{2+} influx, specifically, is involved in the NO-dependent increase of sPSCs, extracellular Ca^{2+} was removed during the application of SNAP. Prior to Ca^{2+} removal, SNAP caused a 61% increase in sPSC frequency (control, 19.4 ± 8.8/30 s, SNAP, 31.2 ± 12.7/30 s, $P = 0.03$, $n = 8$, Fig. 5, *D* and *E*). When extracellular Ca^{2+} was removed during SNAP application, there was a 62% reduction in sPSC frequency (SNAP, 31.2 ± 12.7/30 s, SNAP/0 Ca^{2+}, 11.9 ± 7.1/30 s, $P = 0.02$, $n = 8$, Fig. 5, *D* and *E*). These results indicate that Ca^{2+} influx is required for the NO-dependent increase of sPSC frequency.

Ca^{2+} stores can play a role in vesicle fusion and GABA release in ACs (Chávez et al. 2006, 2010; Ke et al. 2010; Warrier et al. 2005). The contribution of stores to the NO-dependent increase in cytosolic Ca^{2+} was investigated in OGB-loaded ACs that were preincubated with the SERCA pump inhibitor TG (2 μM, 1 h). The effectiveness of this treatment in emptying the Ca^{2+} store was evaluated using caffeine (20 mM) to release store Ca^{2+}. For control cells in 0 $Ca^{2+}{}_{ext}$, caffeine reliably produced rapid increases in cytosolic Ca^{2+} at contact points between processes (0 $Ca^{2+}{}_{ext}$, 12.33 ± 1.21 AU, 0 $Ca^{2+}{}_{ext}$ and caffeine, 13.52 ± 1.14 AU, $P = 0.004$, $n = 25$, Fig. 6, *A–C*). However, cells pretreated with TG did not produce caffeine-dependent Ca^{2+} elevations, indicating depletion of the Ca^{2+} store (Fig. 6, *B* and *D*). Using this same TG pretreatment protocol, the effect of SNAP on cytosolic Ca^{2+} was examined. Under normal external Ca^{2+} conditions, SNAP elicited a 15% and 9% Ca^{2+} elevation in both control (control, 6.2 ± 0.4 AU, SNAP, 7.1 ± 0.5 AU, $P < 0.0001$, $n = 50$, paired *t*-test, Fig. 6, *E* and *G*) and TG-treated (control, 9.4 ± 1.3 AU, SNAP, 10.2 ± 1.2 AU, $P < 0.0001$, $n = 17$, paired *t*-test, Fig. 6, *F* and *H*) cells, respectively. TG-treated cells pro-

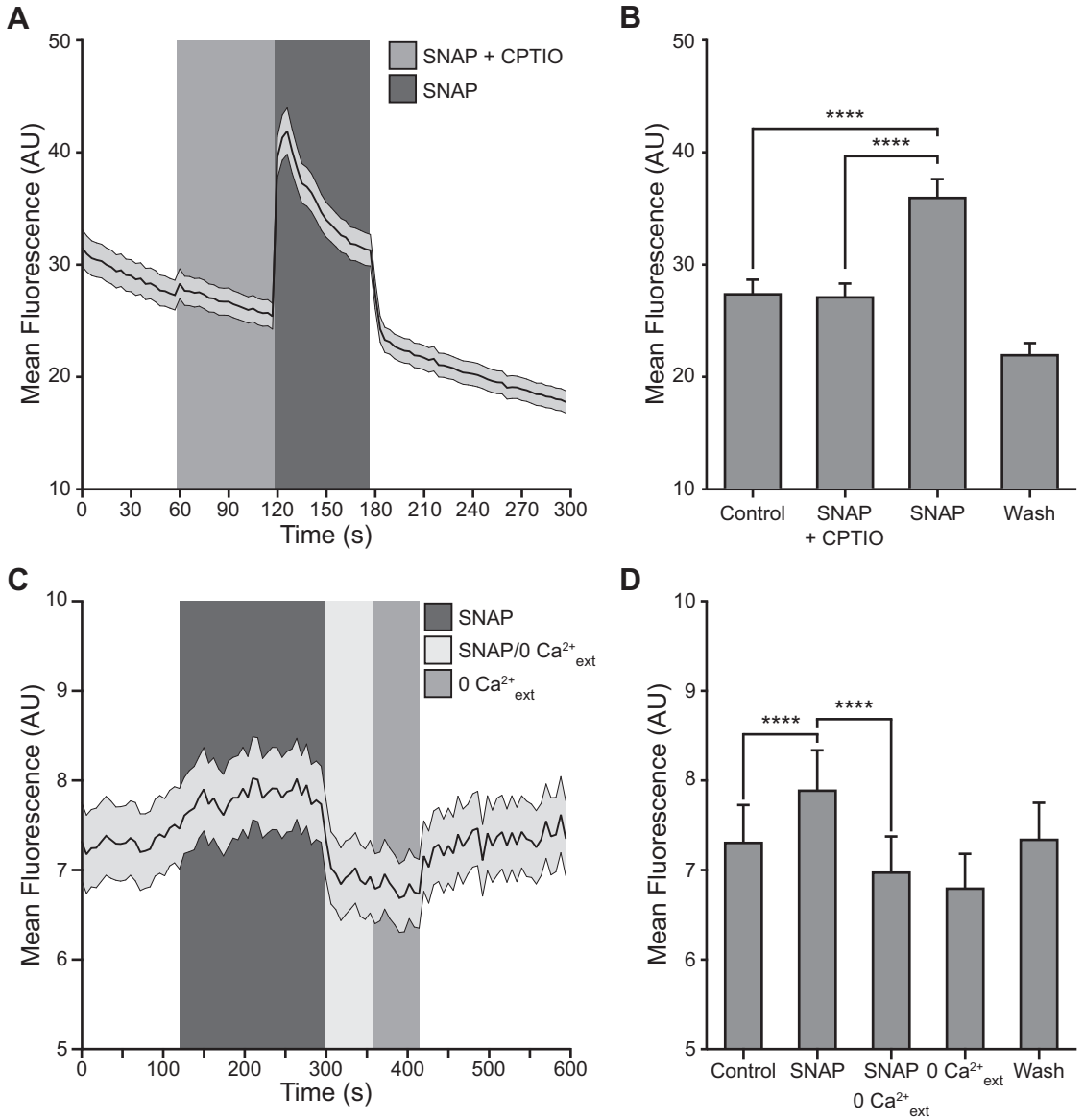

Fig. 4. NO increases intracellular Ca^{2+}. *A*: calcium imaging of AC processes loaded with Oregon Green BAPTA-1 488, AM, revealed that NO caused an increase of intracellular Ca^{2+} at potential synaptic sites. When the NO donor SNAP (500 μM) and NO scavenger CPTIO (10 μM) were coapplied, there was no significant increase in intracellular Ca^{2+} ($P > 0.15$). Removal of CPTIO was followed by a significant increase in cytosolic Ca^{2+}. Note that mean fluorescence in *A* is larger because data were collected with longer exposure times (400 ms) than all other data (200 ms). *B*: quantified mean peak fluorescence ± SE in *A*; $n = 57$. ****$P < 0.0001$ (repeated measures-ANOVA). *C*: intracellular Ca^{2+} is reduced when extracellular Ca^{2+} is removed (0 Ca^{2+}_{ext}), even in the presence of SNAP. *D*: quantified mean peak fluorescence ± SE in *C* showing that SNAP caused a significant increase in fluorescence and that removing extracellular Ca^{2+} (0 Ca^{2+}_{ext}) significantly reduced the fluorescence. $n = 35$. Fluorescence over time data are plotted as mean fluorescence ± SE. ****$P < 0.0001$ (repeated measures-ANOVA).

duced no NO-dependent Ca^{2+} elevations in the absence of extracellular Ca^{2+} (0 Ca^{2+}, 6.9 ± 0.3 AU, 0 Ca^{2+}/SNAP, 6.8 ± 0.3 AU, $P = 0.06$, $n = 107$, Fig. 6, *I* and *J*). These data show that, under these conditions, NO elicits Ca^{2+} elevations by activating a Ca^{2+} influx pathway exclusively.

To confirm that Ca^{2+} stores do not play a role in the NO-dependent increase of sPSCs, voltage clamp recordings were made from ACs preincubated in TG. SNAP still caused a 65% and 171% increase in sPSC frequency in TG-treated (control, 18.3 ± 5.3/30 s, SNAP, 30.2 ± 6.1/30 s, $P = 0.003$, $n = 8$, paired *t*-test, Fig. 7, *B–C*) and in control (control, 10.1 ± 4.1/30 s, SNAP, 27.4 ± 8.3/30 s, $P = 0.034$, $n = 4$, paired *t*-test, Fig. 7, *A* and *C*) cells, respectively. These results confirm that NO increases GABAergic sPSC frequency by activating a plasma membrane Ca^{2+} influx pathway that is independent of Ca^{2+} release from stores.

NO increases evoked GABAergic autaptic transmission. In the retina, ACs receive excitatory signals from bipolar cells. Depolarization of ACs leads to evoked neurotransmitter release onto postsynaptic cells, which can be bipolar cells, ganglion cells or other ACs. To determine the role of NO in evoked neurotransmitter release, perforated patch whole cell recordings were performed on isolated ACs making autapses. Cells were depolarized from −70 mV to −20 mV for 50 ms to activate VGCCs and subsequently cause vesicle fusion and neurotransmitter release. The autaptic currents persisting after

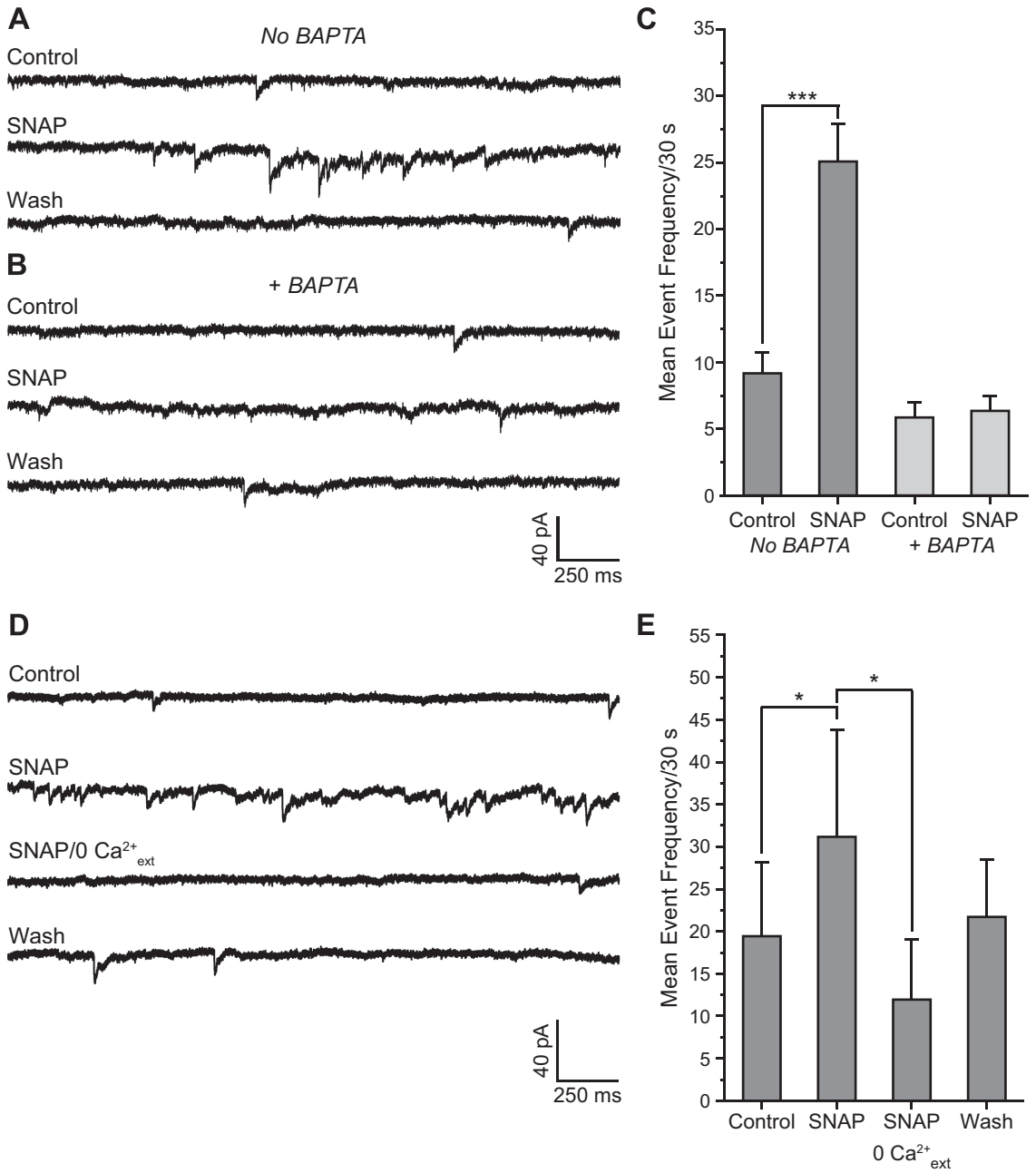

Fig. 5. The NO-dependent increase of sPSC frequency is dependent upon cytosolic Ca^{2+} elevations. *A* and *B*: representative recordings from postsynaptic ACs voltage clamped at −70 mV. *A*: the NO donor SNAP was able to increase sPSC frequency under control conditions (No BAPTA). *B*: in BAPTA-loaded ACs (+BAPTA), however, SNAP did not increase sPSC frequency. *C*: quantified mean event frequency/30 s ± SE. BAPTA-containing cells ($n = 12$) had a significant reduction in control sPSC frequency. The NO-dependent increase in sPSC frequency was significantly reduced in cells containing BAPTA ($n = 12$). ***$P < 0.001$ (paired *t*-test). *D*: recording from a representative AC held at −70 mV. After the removal of extracellular Ca^{2+} (0 Ca^{2+}_{ext}), NO is no longer effective in increasing the frequency of sPSCs. *E*: quantified mean frequency of sPSCs/30 s ± SE; $n = 8$. *$P < 0.05$.

the voltage step were quantified. SNAP caused a 51% increase in charge transfer (control, 177.0 ± 47.6 pC, SNAP, 268.1 ± 59.7 pC, $P = 0.03$, $n = 6$, Fig. 8, *A* and *B*). Bicuculline blocked the NO-dependent increase of the charge transfer (bicuculline, 48.2 ± 13.4 pC, bicuculline/SNAP, 53.1 ± 16.3 pC, $P = 0.32$, $n = 5$, Fig. 8, *C* and *D*). Note that the apparent SNAP-dependent change in the Ca^{2+} current amplitude during the voltage-step is due to the contamination from inward GABA-gated current (Fig. 8*A*), an effect that is absent in the presence of bicuculline (Fig. 8*C*). The sPSC frequency was also elevated during the SNAP application (Fig. 8*A*, *inset*). These data suggest that NO increases evoked GABAergic neurotransmission, possibly due to additive effects of two Ca^{2+} influx pathways being activated (NO-dependent Ca^{2+} influx and voltage-dependent Ca^{2+} influx) simultaneously.

The effect of NO on sPSCs does not involve L-type VGCCs, AMPARs or NMDARs. L-type VGCCs have been demonstrated to mediate neurotransmitter release between these cultured ACs (Gleason et al. 1993) and other AC synapses in the retina (Habermann et al. 2003; Vigh and Lasater 2004). It has also

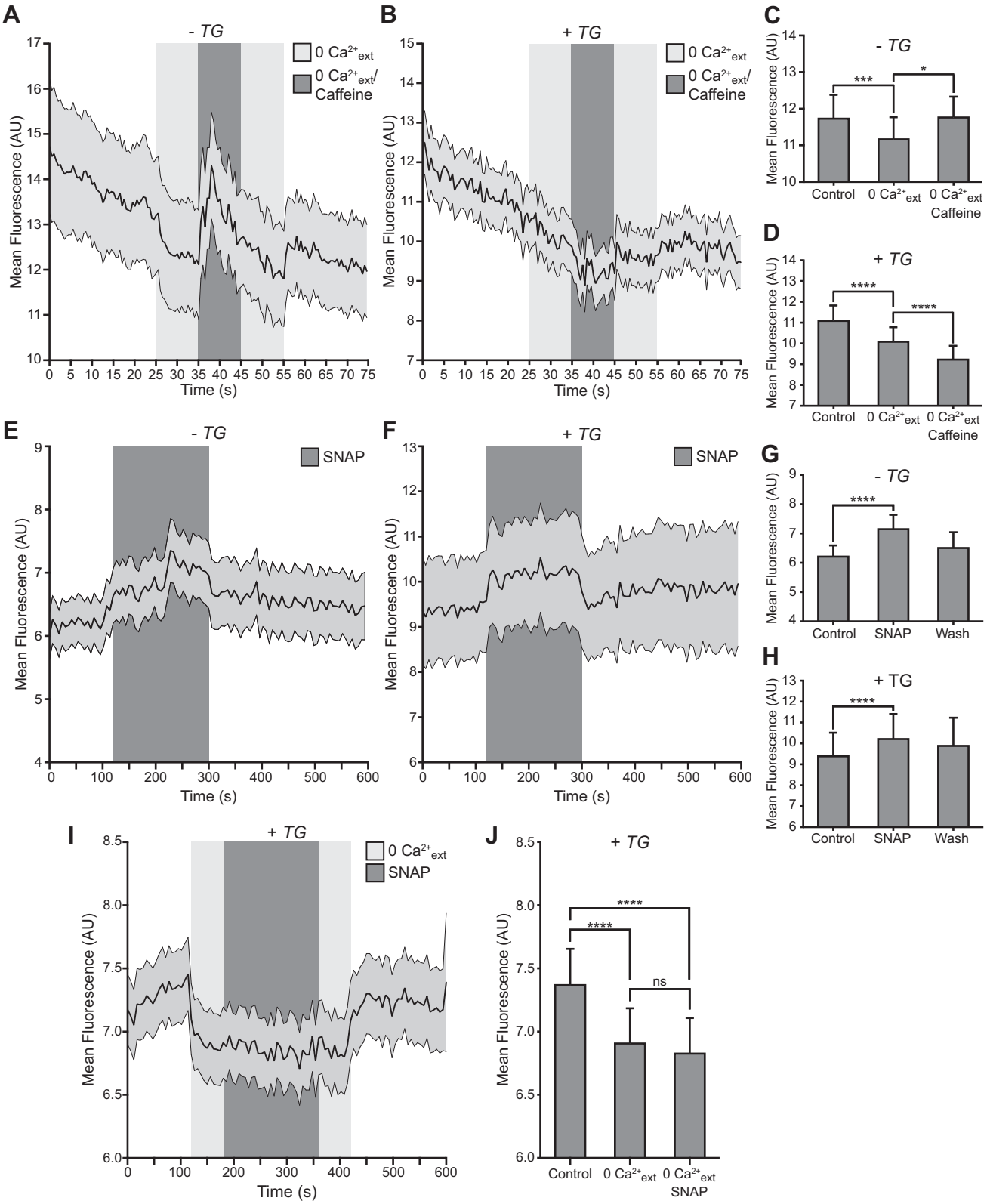

Fig. 6. NO-dependent increase of intracellular Ca^{2+} is independent of intracellular stores. *A*: in the absence of extracellular Ca^{2+} (0 Ca^{2+}_{ext}), caffeine (20 mM) produced a rapid and transient increase in intracellular Ca^{2+} when thapsigargin (TG) was not present. *B*: for cells preincubated in TG (2 μM, 1 h), no caffeine-dependent store release was observed. *C* and *D*: quantified mean fluorescence ± SE in *A* ($n = 25$) and *B* ($n = 37$), respectively. *E* and *F*: the NO donor SNAP produced an increase in intracellular Ca^{2+} in both control and TG-treated AC processes. *G* and *H*: quantified mean fluorescence ± SE in *E* ($n = 50$) and *F* ($n = 107$), respectively. *I*: the NO donor SNAP does not increase intracellular Ca^{2+} in the presence of TG and the absence of extracellular Ca^{2+}. *J*: quantified mean fluorescence ± SE in *I* ($n = 107$). $^{*}P < 0.05$, $^{***}P < 0.001$, $^{****}P < 0.0001$, $^{ns}P > 0.57$ (repeated measures-ANOVA). Fluorescence over time data are plotted as mean fluorescence ± SE.

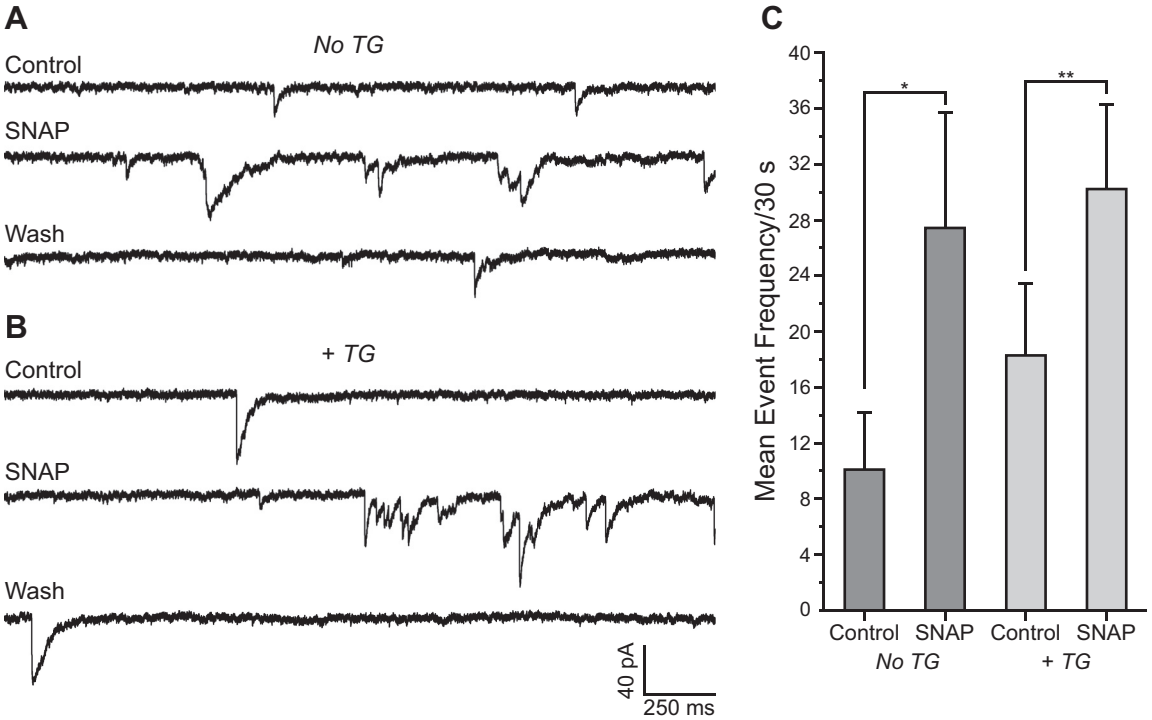

Fig. 7. NO-dependent increase of sPSC frequency is independent of Ca^{2+} stores. *A* and *B*: representative recordings from postsynaptic amacrine ACs held at −70 mV without (*A*) or with (*B*) preincubation with TG (2 μM, 1 h). The NO-dependent increase of sPSC frequency persisted in the presence of TG. *C*: quantified mean event frequency/30 s ± SE. Addition of SNAP increased sPSCs in cells with intact Ca^{2+} stores (No TG; dark shaded bars, $n = 4$) and after Ca^{2+} store depletion (+TG; light shaded bars, $n = 8$). $^*P < 0.05$, $^{**}P < 0.01$ (paired *t*-tests).

been demonstrated that NO can activate retinal ganglion cell Ca^{2+} channels (Hirooka et al. 2000) and augment neuronal L-type Ca^{2+} currents (Tozer et al. 2012). To determine if NO has an effect on the voltage-gated Ca^{2+} current or activation voltage, voltage ramps from −90 mV to +50 mV were delivered in the presence of TTX (300 nM) and bicuculline (10 μM) to isolate the Ca^{2+} current. In these experiments, perforated-patch normal internal solution and TEA-Cl external solution were used. Addition of SNAP did not change the Ca^{2+} current amplitude (control, −268.9 ± 45.1 pA, SNAP, −261.2 ± 43.8 pA, $P = 0.45$, $n = 9$, Fig. 9*A*) or the Ca^{2+} channel activation voltage (control, −45.36 ± 1.1 mV, SNAP, −45.13 ± 0.73 mV, $P = 0.69$, $n = 9$). Additionally, the L-type VGCC inhibitor nifedipine (20 μM) did not prevent the NO-dependent increase in sPSC frequency (nifedipine, 20.40 ± 4.2/30 s, nifedipine/SNAP, 37.65 ± 6.07/30 s, $P = 0.028$, $n = 5$, Fig. 9, *B* and *C*). The NO-dependent increase in sPSC frequency remained unchanged after removal of nifedipine and leaving only SNAP in the bath (nifedipine/SNAP, 37.65 ± 6.07/30 s, SNAP, 40.3 ± 8.98/30 s, $P = 0.78$, $n = 5$). These results demonstrate that L-type VGCCs are not involved. The possibility that NO could activate α-amino-3-hydroxy-5-methyl-4-isoxazolepropionic acid (AMPA) and/or *N*-methyl-D-aspartate (NMDA) glutamate receptors (AMPARs and NMDARs) was investigated using Ca^{2+} imaging. The AMPAR and NMDAR antagonists CNQX (50 μM) and D-AP5 (10 μM), respectively, were applied before and during the application of SNAP. While AMPRs and NMDARs were blocked, NO increased intracellular Ca^{2+} by 10.8% (D-AP5/CNQX, 8.1 ± 0.3 AU, D-AP5/CNQX and SNAP, 8.9 ± 0.4 AU, $n = 152$ ROIs, $P < 0.0001$, Fig. 9*D*). When D-AP5 and CNQX were removed, intracellular Ca^{2+} remained elevated (D-AP5/CNQX and SNAP, 8.9 ± 0.4 AU, SNAP, 9.1 ± 0.4 AU, $n = 152$ ROIs, $P = 0.1$). These results show that NO does not activate L-type VGCCs, AMPARs or NMDARs. Therefore, NO must be activating another plasma membrane Ca^{2+} influx pathway to admit extracellular Ca^{2+} presynaptically and to increase sPSC frequency.

Clemizole blocks the NO-dependent increase in sPSC frequency and intracellular Ca^{2+}. Previous work in our laboratory demonstrated that these ACs contain mRNA for TRPC subunits 1, 3, 4, 5, 6, and 7 (Crousillac et al. 2003), and TRPC channels can be activated via *S*-nitrosylation (Yoshida et al. 2006). To explore the possible role of TRPC channels in the NO-dependent increase in sPSC frequency, we used two traditional TRPC inhibitors, 2-APB and SKF96365. These inhibitors, however, have multiple documented effects on other ion channels, some of which conduct Ca^{2+} (DeHaven et al. 2008; Hong et al. 1994; Hotta et al. 2005; Leung et al. 1996; Merritt et al. 1990; Prakriya and Lewis 2001; Singh et al. 2010; Usmani et al. 2010; Wang 2003). Application of 2-APB (20 μM) alone increased sPSC frequency from baseline by 108% (control, 52 ± 7.5/30 s, 2-APB, 107.9 ± 15.3/30 s, $P = 0.01$, $n = 10$, paired *t*-test), and application of SKF96365 (30 μM) alone increased sPSC frequency from baseline by 431% (control, 33.4 ± 7.5/30 s, SKF96365, 177.4 ± 44.3 s, $P = 0.044$, $n = 4$, paired *t*-test). To avoid these confounding effects, clemizole (10 μM), a more specific TRPC channel blocker (with highest selectivity for TRPC5), was utilized to investigate TRPC channel involvement in the NO-dependent response. In the presence of clemizole, SNAP was unable to increase sPSC frequency (control, 17.2 ± 3.7/30 s, clemizole/SNAP, 17.9 ± 2.0/30 s, $P = 0.84$, $n = 10$, Fig. 10, *A* and *B*). When clemizole was removed, SNAP increased sPSC fre-

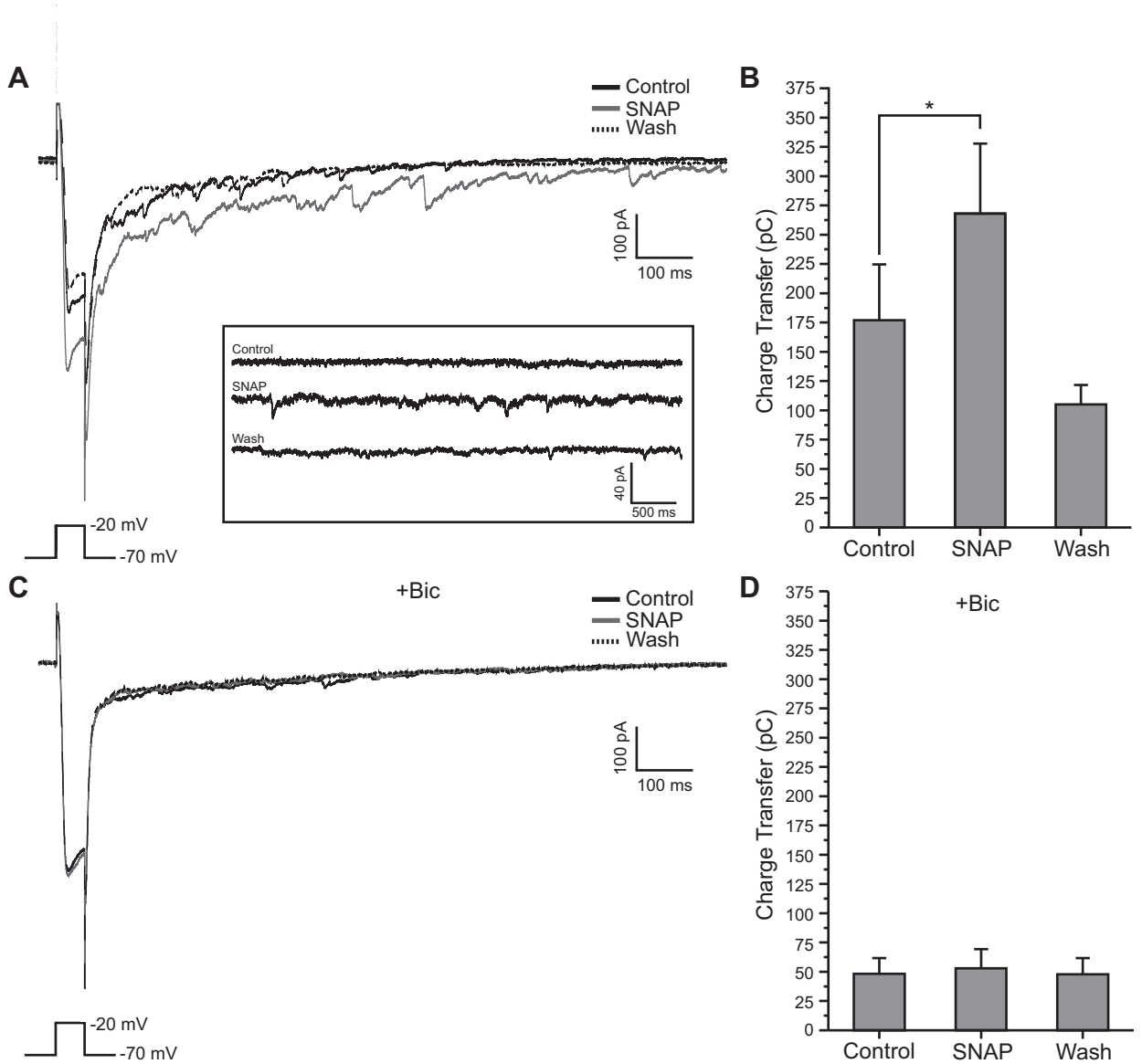

Fig. 8. NO increases evoked autaptic GABAergic postsynaptic currents. *A*: recording from a representative AC depolarized from −70 mV to −20 mV for 50 ms. Evoked autaptic currents were increased after the addition of the NO donor SNAP. *Inset*: sPSC frequency was elevated between depolarizations during the application of SNAP. *B*: quantified mean charge transfer ± SE; $n = 6$. *$P < 0.05$ (paired *t*-test). *C*: recording from a representative AC depolarized from −70 mV to −20 mV for 50 ms. Addition of the $GABA_A$ receptor antagonist bicuculline blocked the NO-dependent increase of charge transfer. *D*: quantified mean charge transfer ± SE; $n = 5$. The NO donor SNAP did not significantly alter the evoked autaptic currents in the presence of bicuculline. $P > 0.3$ (paired *t*-test).

quency by 203% (clemizole/SNAP, 17.9 ± 2/30 s, SNAP, 54.1 ± 16.8/30 s, $P = 0.04$, $n = 10$, Fig. 10, *A* and *B*). Additionally, SNAP was unable to increase process intracellular Ca^{2+} in the presence of clemizole (clemizole, 5.7 ± 0.4 AU, clemizole/SNAP, 5.7 ± 0.4 AU, $P = 0.45$, $n = 46$ ROIs, Fig. 10, *C* and *D*). When clemizole was removed, SNAP increased intracellular Ca^{2+} by 7% (clemizole/SNAP, 5.7 ± 0.4 AU, SNAP, 6.1 ± 0.4 AU, $P < 0.0001$, $n = 46$, Fig. 10, *C* and *D*). Clemizole is also able to block H1 histamine receptors (Aguilar et al. 1986). It has been demonstrated that these receptors are functionally expressed in rodent dopaminergic ACs, and that their activation can engender Ca^{2+} elevations (Frazão et al. 2011; Gastinger et al. 2006). Although the ACs in our cultures are GABAergic, we tested whether histamine (10 μM and 100 μM) produced Ca^{2+} elevations. We found that Ca^{2+} elevations were not elicited by 10 μM histamine (control, 5.09 ± 0.25 AU, 10 μM histamine, 5.05 ± 0.26 AU, $P = 0.16$, $n = 48$) or 100 μM histamine (control, 4.05 ± 0.12 AU, 100 μM histamine, 4.07 ± 0.12 AU, $P = 0.19$, $n = 216$), suggesting either that histamine receptors are not expressed, or that their activation is not linked to an increase in cytosolic Ca^{2+}. Together, these results provide evidence that NO increases GABA release from ACs by activating a TRPC-mediated Ca^{2+} influx.

DISCUSSION

These results demonstrate that NO promotes neurotransmitter release at GABAergic synapses in retinal amacrine cells (ACs). We find that this action of NO is not dependent on presynaptic APs or sGC activity; however, it is dependent upon

an elevation in cytosolic Ca^{2+}. Both NO-dependent Ca^{2+} elevations and NO-dependent increases in sPSCs were unaffected by store depletion, indicating that Ca^{2+} influx alone mediates the effects of NO. Evoked GABA release was also enhanced in the presence of NO, but the activation of VGCCs was unaffected by NO. Together, these observations imply that, during evoked release, the NO-dependent Ca^{2+} elevations can add to the voltage-dependent Ca^{2+} elevations to enhance the evoked release of GABA. This interpretation is consistent with the steep dependence of evoked neurotransmitter release on Ca^{2+} (Augustine and Charlton 1986; Dodge and Rahamimoff 1967; Reid et al. 2003). Blocking TRPC channels using clemizole prevented the NO-dependent increase in sPSC frequency and intracellular Ca^{2+}. These results suggest that NO activates a TRPC-mediated Ca^{2+} influx pathway that is sufficient to drive synaptic exocytosis.

VGCC-independent GABA release. Other mechanisms of VGCC-independent GABA release have been demonstrated in ACs. Chávez et al. (2006) showed that, in the rat retina, reciprocal GABAergic synapses from A17 ACs onto bipolar cells can be directly stimulated by the activation of Ca^{2+}-permeable AMPA receptors. Voltage-independent GABA release was also demonstrated for cultured chick ACs via activation of metabotropic glutamate receptor 5 (Warrier et al. 2005). Both of these mechanisms involved amplification through release of Ca^{2+} from stores. Additionally, a study of unstimulated GABA release from cultured rat ACs demonstrated the involvement of both Ca^{2+} influx and store release (Ke et al. 2010). The NO-dependent increase in sPSCs reported here is novel because our results argue against a contribution from stores.

NO and GABA release. In agreement with our finding in cultured ACs, experiments measuring the levels of a GABA analog loaded in slices of turtle retina showed that NO promoted GABA release from ACs as well as HCs (Yu and Eldred 2005). Significantly, in the inner retina where ACs signal, the NO-dependent increase in GABA release was largely Ca^{2+} dependent and sGC independent, consistent with what we find for cultured ACs. NO has also been reported to stimulate GABA release from GABAergic cells in the ganglion cell layer (most likely displaced ACs) (Maggesissi et al. 2009) in the intact chicken retina, although the underlying mechanism was not investigated. Previous studies measuring the effects of NO on GABA release at other central synapses have demonstrated both enhancement (Merino et al. 2014; Tarasenko et al. 2014) and inhibition (De Laurentiis et al. 2000; Wall 2003). In studies of the effects of NO on GABAergic sPSC frequency specifically, both increases in sPSC frequency (Li et al. 2002, 2004; Xing et al. 2008; Yang and Cox 2007) and decreases in sPSC frequency (Lee 2009) have been reported for central mammalian synapses. Both of these effects can be dependent upon sGC activity (Lee 2009; Li et al. 2004; Yang and Cox 2007). Here, we show that GABAergic sPSC frequency is enhanced by NO via a sGC-independent mechanism. Together, these studies establish that the effects of NO on GABAergic signaling can be functionally and mechanistically diverse, indicating

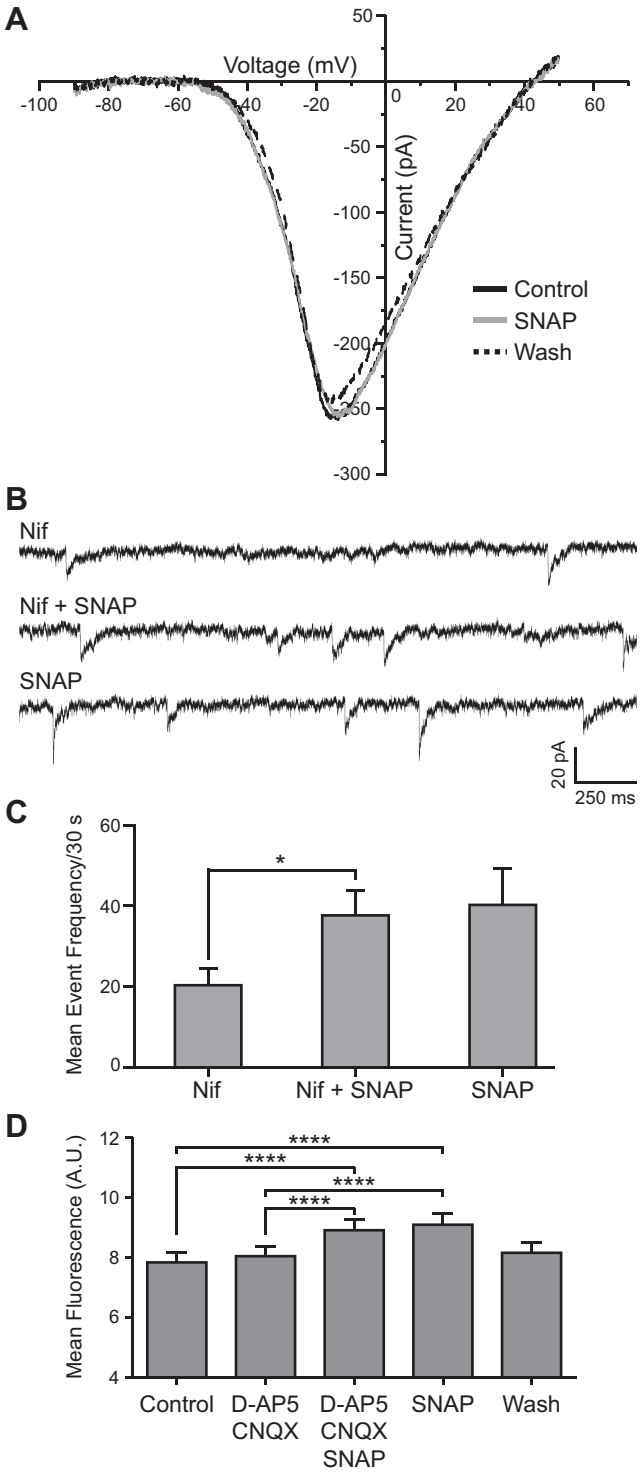

Fig. 9. L-type voltage-gated Ca^{2+} channels (VGCCs), AMPARs or NMDARs are not required for the NO-dependent Ca^{2+} influx. *A*: voltage clamp recording from a representative AC ramped from −90 mV to 50 mV. The NO donor SNAP (500 μM) did not affect the activation voltage or the peak of the Ca^{2+} current. Bicuculline and TTX were included in the TEA-Cl external solution to isolate the Ca^{2+} current. *B*: current recording from a representative amacrine cell voltage clamped at −70 mV. SNAP still increased sPSC frequency in the presence of the L-type VGCC inhibitor nifedipine (Nif, 20 μM). sPSC frequency was unchanged after removal of Nif. *C*: quantified mean event frequency/30 s ± SE; $n = 5$. *$P < 0.05$ (repeated measures-ANOVA). *D*: the NO-dependent influx of Ca^{2+} still occurred in the presence of the NMDAR inhibitor D-AP5 (10 μM) and the AMPAR inhibitor CNQX (50 μM). Data are mean fluorescence (AU) ± SE; $n = 152$ ROIs. ****$P < 0.0001$ (repeated measures-ANOVA).

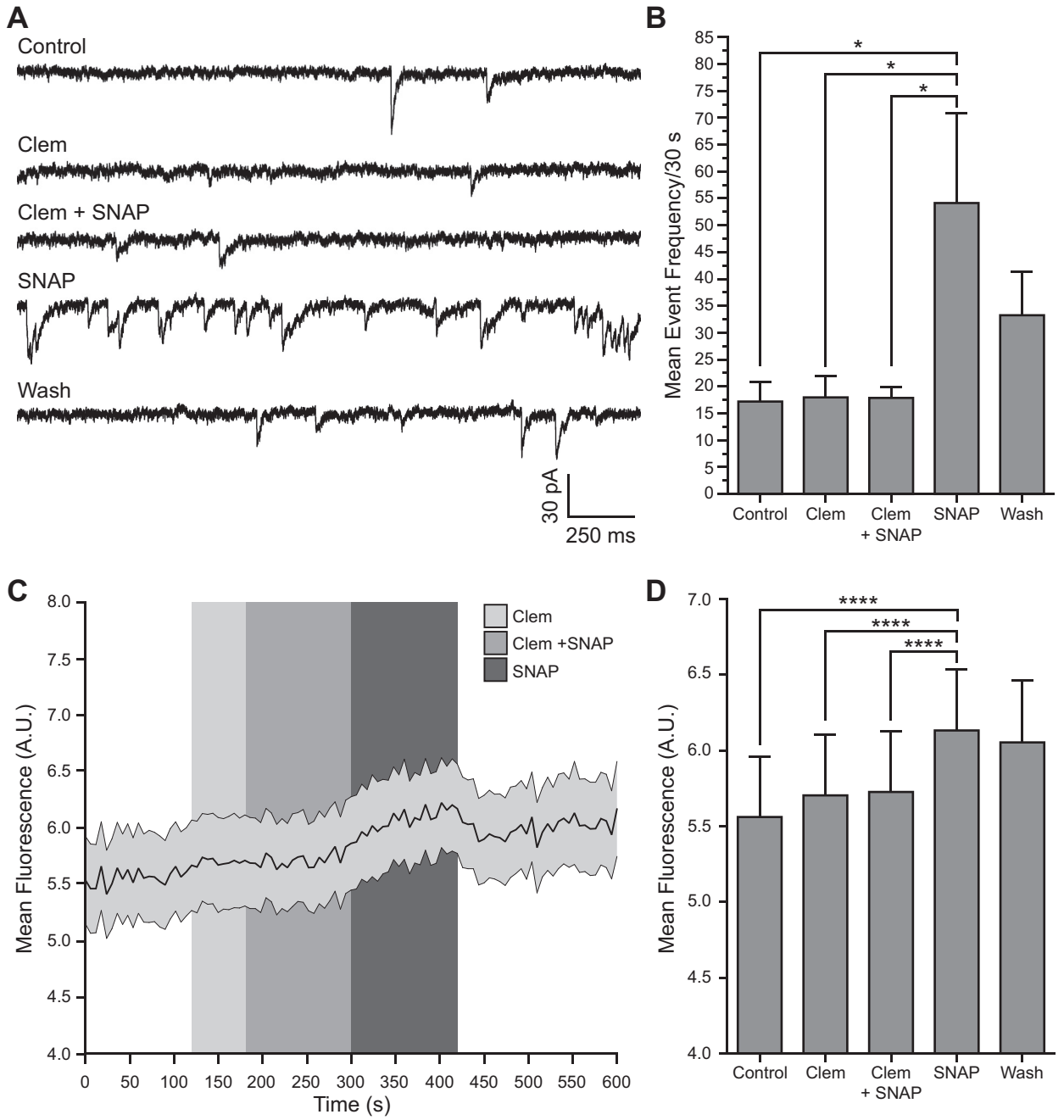

Fig. 10. Clemizole (clem) blocks the NO-dependent increase in sPSC frequency and intracellular Ca^{2+}. *A*: current recording from a representative amacrine cell voltage clamped at −70 mV. Application of the TRPC inhibitor clem (10 μM) and coapplication of clem and the NO donor SNAP (500 μM) did not alter sPSC frequency. Removal of clem from the bath leaving only SNAP caused an increase in sPSC frequency. *B*: quantified mean event frequency/30 s ± SE; $n = 10$. *$P < 0.05$ (repeated measures-ANOVA). *C*: SNAP was unable to increase intracellular Ca^{2+} during the application of clem; however, SNAP increased intracellular Ca^{2+} upon removal of clem. *D*: quantified mean fluorescence ± SE; $n = 46$. ****$P < 0.0001$ (repeated measures-ANOVA). Fluorescence over time data are plotted as mean fluorescence ± SE.

that the effects of NO on the synaptic output of any one class of neuron is not predictable.

Role of spontaneous GABA release. There is abundant evidence that spontaneous and AP-evoked vesicular neurotransmitter release occur by distinct processes that involve different Ca^{2+} sensitivities, molecular machinery and synaptic vesicle pools (Kavalali 2015; Smith et al. 2012). This existence of a parallel and similarly complex system of neurotransmitter release implies that spontaneous release has distinctive functions. One emerging role is in the regulation of the synapse itself. Most is known about the role of spontaneous glutamate release in regulating synaptic function; however, recent work has demonstrated that spontaneous GABA release regulates synaptic scaling in the embryonic chick spinal cord (Garcia-Bereguiain et al. 2016). The mechanism underlying this action of GABA depends on the depolarizing effect of GABA at that time in development, and scaling is achieved by further adjusting the level of postsynaptic Cl^-. Our laboratory has previously demonstrated that NO can release Cl^- from an internal store and transiently convert inhibitory GABAergic synapses

into excitatory GABAergic synapses (Hoffpauir et al. 2006; Krishnan and Gleason 2015). Thus the ability of GABA to even transiently generate depolarization-dependent Ca^{2+} elevations opens up the possibility that NO-dependent spontaneous activity at AC synapses can further modulate their own synaptic function.

TRPCs in ACs. Our experiments with clemizole suggest that TRPC channels are induced to admit presynaptic Ca^{2+} by NO. There is additional evidence in the literature suggesting the functional expression of TRPC channels in ACs. In cultured rat ACs, the broad TRPC channel inhibitor SKF96365 reduced GABAergic sPSC frequency, suggesting TRPC channels play a role in synaptic output (Ke et al. 2010). In our experiments, SKF96365 caused an increase in sPSC frequency. In cultured chick ACs, 2-APB was used to inhibit activation of inositol 1,4,5-trisphosphate receptors, which prevented both a depolarization- and mGluR5-dependent increase in sPSC frequency (Warrier et al. 2005). Here (in the absence of depolarization or mGluR5 activation), 2-APB caused an increase in sPSC frequency. Having multiple sites of action (DeHaven et al. 2008; Hong et al. 1994; Hotta et al. 2005; Leung et al. 1996; Merritt et al. 1990; Prakriya and Lewis 2001; Singh et al. 2010; Usmani et al. 2010; Wang 2003), SKF96365 and 2-APB are problematic in investigating the involvement of TRPC channels in the NO-dependent increase in intracellular Ca^{2+} and GABAergic sPSC frequency in cultured ACs. The more specific TRPC inhibitor clemizole did not activate spontaneous release on its own, but it was effective in suppressing the effects of NO. Clemizole is most selective for TRPC5 (IC_{50} = 1.1 μM), however, it can also inhibit TRPC4 (IC_{50} = 6.4 μM), TRPC3 (IC_{50} = 9.1 μM), TRPC6 (IC_{50} = 11.3 μM) and TRPC7 (IC_{50} 26.5 μM) (Richter et al. 2014). Interestingly, homomeric TRPC1, TRPC5, or heteromeric TRPC1/5 channels can be activated by *S*-nitrosylation (Yoshida et al. 2006). The effects of the *S*-nitrosylation inhibitor NEM alone, however, precluded our use of this reagent to assess the role of this modification. Transcripts encoding TRPCs 1 and 3–7 have been RT-PCR amplified from pools of 10–20 cultured ACs (Crousillac et al. 2009). There is also immunocytochemical evidence that TRPC1 is expressed by ACs in the chicken retina and can colocalize with nNOS (Crousillac et al. 2003). The TRPC channel (s) involved in the NO-dependent increase in intracellular Ca^{2+} and sPSC frequency remains to be elucidated.

Multiple effects of NO on AC synapses. As mentioned above, we have shown that NO can transiently alter the postsynaptic responses of ACs by releasing Cl^- from internal acidic compartments (Hoffpauir et al. 2006; Krishnan and Gleason 2015). This increase in cytosolic Cl^- makes the reversal potential of both GABA- and glycine-gated currents more positive, such that synaptic voltage responses temporarily become less inhibitory or even excitatory. This change can shift the balance of excitatory and inhibitory input at a synaptic site and increase synaptic output (Fig. 11). Here, we show that NO also acts on the presynaptic side of AC GABAergic synapses by activating a TRPC-mediated Ca^{2+} influx pathway that is sufficient to drive exocytosis in the absence of depolarization. Taken together, these results suggest that, in the inner retina, locally generated NO can affect both pre- and postsynaptic sites. GABA release is enhanced, and GABA action on the postsynaptic cell can lead to depolarization. If these actions co-occur, as depicted in Fig. 11, then they will enhance inhibitory output from the downstream AC. Ultimately, the patterns of NO production under different stimulus conditions will determine the sites of enhanced GABAergic output and thus the impact on the signals that ganglion cells send to visual centers in the brain.

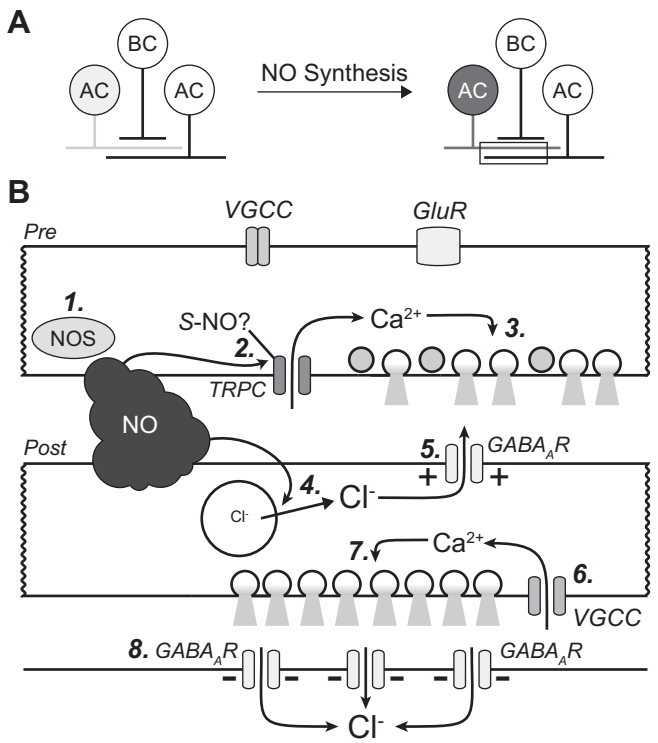

Fig. 11. NO has pre- and postsynaptic effects in ACs. *A*, *left*: simplified cartoon of a GABAergic AC (light shading) in the retina receiving excitatory glutamatergic input from a bipolar cell (BC) and presynaptic to another AC. *Right*: NO synthesis in a NOS expressing AC (dark shading) can elicit changes in both pre- and postsynaptic processes. *B*: expanded view of the box in *A*, depicting presynaptic and postsynaptic effects of NO. *Top*: activation of a Ca^{2+}-dependent isoform of NOS (eNOS or nNOS) produces NO (*1*). NO activates a voltage-independent Ca^{2+}-permeable plasma membrane channel, possibly via *S*-nitrosylation (*S*-NO?) of a TRPC channel, to admit Ca^{2+} into the presynaptic terminal (*2*). Ca^{2+} elevations in the presynaptic terminal lead to increased vesicle fusion events and GABA release (*3*) onto its postsynaptic partner. VGCC, voltage-gated Ca^{2+} channel; GluR, ionotropic glutamate receptor. *Bottom*: NO diffuses into the postsynaptic terminal and induces Cl^- release from acidic organelles (*4*) (Krishnan and Gleason 2015). Increased Cl^- concentration in the postsynaptic terminal reverses the Cl^- gradient, converting typical GABAergic inhibition into depolarization (*5*) (Hoffpauir et al. 2006). Depolarization (+) leads to activation of VGCCs in an adjacent presynaptic site in the same process (*6*). Ca^{2+} influx through activated VGCCs leads to enhanced GABA release (*7*). The postsynaptic partner that is downstream from the targets of NO will experience increased inhibition (*8*).

ACKNOWLEDGMENTS

We thank S. Crousillac for critical reading of the manuscript.

GRANTS

This work was supported by a Sigma Xi Grant-in-Aid of Research to J. W. M. and National Science Foundation Grant 1256782 to E. G.

DISCLOSURES

No conflicts of interest, financial or otherwise, are declared by the author(s).

AUTHOR CONTRIBUTIONS

J.W.M. and E.L.G. conceived and designed research; J.W.M. performed experiments; J.W.M. analyzed data; J.W.M. and E.L.G. interpreted results of experiments; J.W.M. prepared figures; J.W.M. and E.L.G. drafted manuscript; J.W.M. and E.L.G. edited and revised manuscript; J.W.M. and E.L.G. approved final version of manuscript.

REFERENCES

Aguilar MJ, Morales-Olivas FJ, Rubio E. Pharmacological investigation into the effects of histamine and histamine analogues on guinea-pig and rat colon in vitro. *Br J Pharmacol* 88: 501–506, 1986. doi:10.1111/j.1476-5381.1986.tb10229.x.

Augustine GJ, Charlton MP. Calcium dependence of presynaptic calcium current and post-synaptic response at the squid giant synapse. *J Physiol* 381: 619–640, 1986. doi:10.1113/jphysiol.1986.sp016347.

Bindoli A, Fleischer S. Induced Ca2+ release in skeletal muscle sarcoplasmic reticulum by sulfhydryl reagents and chlorpromazine. *Arch Biochem Biophys* 221: 458–466, 1983. doi:10.1016/0003-9861(83)90164-9.

Blom J, Giove T, Deshpande M, Eldred WD. Characterization of nitric oxide signaling pathways in the mouse retina. *J Comp Neurol* 520: 4204–4217, 2012. doi:10.1002/cne.23148.

Cao L, Eldred WD. Subcellular localization of neuronal nitric oxide synthase in turtle retina: electron immunocytochemistry. *Vis Neurosci* 18: 949–960, 2001.

Chávez AE, Grimes WN, Diamond JS. Mechanisms underlying lateral GABAergic feedback onto rod bipolar cells in rat retina. *J Neurosci* 30: 2330–2339, 2010. doi:10.1523/JNEUROSCI.5574-09.2010.

Chávez AE, Singer JH, Diamond JS. Fast neurotransmitter release triggered by Ca influx through AMPA-type glutamate receptors. *Nature* 443: 705–708, 2006. doi:10.1038/nature05123.

Clary DO, Griff IC, Rothman JE. SNAPs, a family of NSF attachment proteins involved in intracellular membrane fusion in animals and yeast. *Cell* 61: 709–721, 1990. doi:10.1016/0092-8674(90)90482-T.

Cook PB, Lukasiewicz PD, McReynolds JS. Action potentials are required for the lateral transmission of glycinergic transient inhibition in the amphibian retina. *J Neurosci* 18: 2301–2308, 1998.

Crousillac S, Colonna J, McMains E, Dewey JS, Gleason E. Sphingosine-1-phosphate elicits receptor-dependent calcium signaling in retinal amacrine cells. *J Neurophysiol* 102: 3295–3309, 2009. doi:10.1152/jn.00119.2009.

Crousillac S, LeRouge M, Rankin M, Gleason E. Immunolocalization of TRPC channel subunits 1 and 4 in the chicken retina. *Vis Neurosci* 20: 453–463, 2003. doi:10.1017/S0952523803204107.

De Laurentiis A, Pisera D, Duvilanski B, Rettori V, Lasaga M, Seilicovich A. Neurokinin A inhibits oxytocin and GABA release from the posterior pituitary by stimulating nitric oxide synthase. *Brain Res Bull* 53: 325–330, 2000. doi:10.1016/S0361-9230(00)00356-7.

DeHaven WI, Smyth JT, Boyles RR, Bird GS, Putney JW Jr. Complex actions of 2-aminoethyldiphenyl borate on store-operated calcium entry. *J Biol Chem* 283: 19265–19273, 2008. doi:10.1074/jbc.M801535200.

DeVries SH, Schwartz EA. Modulation of an electrical synapse between solitary pairs of catfish horizontal cells by dopamine and second messengers. *J Physiol* 414: 351–375, 1989. doi:10.1113/jphysiol.1989.sp017692.

Dodge FA Jr, Rahamimoff R. Co-operative action a calcium ions in transmitter release at the neuromuscular junction. *J Physiol* 193: 419–432, 1967. doi:10.1113/jphysiol.1967.sp008367.

Eldred WD, Blute TA. Imaging of nitric oxide in the retina. *Vision Res* 45: 3469–3486, 2005. doi:10.1016/j.visres.2005.07.033.

Euler T, Detwiler PB, Denk W. Directionally selective calcium signals in dendrites of starburst amacrine cells. *Nature* 418: 845–852, 2002. doi:10.1038/nature00931.

Fischer AJ, Stell WK. Nitric oxide synthase-containing cells in the retina, pigmented epithelium, choroid, and sclera of the chick eye. *J Comp Neurol* 405: 1–14, 1999. doi:10.1002/(SICI)1096-9861(19990301)405:1<1::AID-CNE1>3.0.CO;2-U.

Frazão R, McMahon DG, Schunack W, Datta P, Heidelberger R, Marshak DW. Histamine elevates free intracellular calcium in mouse retinal dopaminergic cells via H1-receptors. *Invest Ophthalmol Vis Sci* 52: 3083–3088, 2011. doi:10.1167/iovs.10-6160.

Garcia-Bereguiain MA, Gonzalez-Islas C, Lindsly C, Wenner P. Spontaneous release regulates synaptic scaling in the embryonic spinal network in vivo. *J Neurosci* 36: 7268–7282, 2016. doi:10.1523/JNEUROSCI.4066-15.2016.

Gastinger MJ, Barber AJ, Vardi N, Marshak DW. Histamine receptors in mammalian retinas. *J Comp Neurol* 495: 658–667, 2006. doi:10.1002/cne.20902.

Gleason E, Borges S, Wilson M. Synaptic transmission between pairs of retinal amacrine cells in culture. *J Neurosci* 13: 2359–2370, 1993.

Graham S, Ding M, Ding Y, Sours-Brothers S, Luchowski R, Gryczynski Z, Yorio T, Ma H, Ma R. Canonical transient receptor potential 6 (TRPC6), a redox-regulated cation channel. *J Biol Chem* 285: 23466–23476, 2010. doi:10.1074/jbc.M109.093500.

Grimes WN, Zhang J, Graydon CW, Kachar B, Diamond JS. Retinal parallel processors: more than 100 independent microcircuits operate within a single interneuron. *Neuron* 65: 873–885, 2010. doi:10.1016/j.neuron.2010.02.028.

Grimes WN, Zhang J, Tian H, Graydon CW, Hoon M, Rieke F, Diamond JS. Complex inhibitory microcircuitry regulates retinal signaling near visual threshold. *J Neurophysiol* 114: 341–353, 2015. doi:10.1152/jn.00017.2015.

Habermann CJ, O'Brien BJ, Wässle H, Protti DA. AII amacrine cells express L-type calcium channels at their output synapses. *J Neurosci* 23: 6904–6913, 2003.

Haverkamp S, Kolb H, Cuenca N. Morphological and neurochemical diversity of neuronal nitric oxide synthase-positive amacrine cells in the turtle retina. *Cell Tissue Res* 302: 11–19, 2000. doi:10.1007/s004410000267.

Heflin SJ, Cook PB. Narrow and wide field amacrine cells fire action potentials in response to depolarization and light stimulation. *Vis Neurosci* 24: 197–206, 2007. doi:10.1017/S095252380707040X.

Hirooka K, Kourennyi DE, Barnes S. Calcium channel activation facilitated by nitric oxide in retinal ganglion cells. *J Neurophysiol* 83: 198–206, 2000.

Hoffpauir B, McMains E, Gleason E. Nitric oxide transiently converts synaptic inhibition to excitation in retinal amacrine cells. *J Neurophysiol* 95: 2866–2877, 2006. doi:10.1152/jn.01317.2005.

Hong SJ, Lin WW, Chang CC. Inhibition of the sodium channel by SK&F 96365, an inhibitor of the receptor-operated calcium channel, in mouse diaphragm. *J Biomed Sci* 1: 172–178, 1994. doi:10.1007/BF02253347.

Hotta A, Kim YC, Nakamura E, Kito Y, Yamamoto Y, Suzuki H. Effects of inhibitors of nonselective cation channels on the acetylcholine-induced depolarization of circular smooth muscle from the guinea-pig stomach antrum. *J Smooth Muscle Res* 41: 313–327, 2005. doi:10.1540/jsmr.41.313.

Kavalali ET. The mechanisms and functions of spontaneous neurotransmitter release. *Nat Rev Neurosci* 16: 5–16, 2015. doi:10.1038/nrn3875.

Ke JB, Chen W, Yang XL, Wang Z. Characterization of spontaneous inhibitory postsynaptic currents in cultured rat retinal amacrine cells. *Neuroscience* 165: 395–407, 2010. doi:10.1016/j.neuroscience.2009.10.010.

Kim IB, Lee EJ, Kim KY, Ju WK, Oh SJ, Joo CK, Chun MH. Immunocytochemical localization of nitric oxide synthase in the mammalian retina. *Neurosci Lett* 267: 193–196, 1999. doi:10.1016/S0304-3940(99)00363-8.

Kim KY, Ju WK, Oh SJ, Chun MH. The immunocytochemical localization of neuronal nitric oxide synthase in the developing rat retina. *Exp Brain Res* 133: 419–424, 2000. doi:10.1007/s002210000419.

Kirmse K, Kirischuk S. *N*-ethylmaleimide increases release probability at GABAergic synapses in layer I of the mouse visual cortex. *Eur J Neurosci* 24: 2741–2748, 2006. doi:10.1111/j.1460-9568.2006.05179.x.

Knight D, Bellingham MC, Lavidis NA. The effect of *N*-ethylmaleimide on transmitter release from the skeletal neuromuscular junction of *Bufo marinus*. *Synapse* 53: 151–158, 2004. doi:10.1002/syn.20044.

Krishnan V, Gleason E. Nitric oxide releases Cl(-) from acidic organelles in retinal amacrine cells. *Front Cell Neurosci* 9: 213, 2015. doi:10.3389/fncel.2015.00213.

Lee JJ. Nitric oxide modulation of GABAergic synaptic transmission in mechanically isolated rat auditory cortical neurons. *Korean J Physiol Pharmacol* 13: 461–467, 2009. doi:10.4196/kjpp.2009.13.6.461.

Leung YM, Kwan CY, Loh TT. Dual effects of SK&F 96365 in human leukemic HL-60 cells. Inhibition of calcium entry and activation of a novel cation influx pathway. *Biochem Pharmacol* 51: 605–612, 1996. doi:10.1016/S0006-2952(95)02181-7.

Li DP, Chen SR, Finnegan TF, Pan HL. Signalling pathway of nitric oxide in synaptic GABA release in the rat paraventricular nucleus. *J Physiol* 554: 100–110, 2004. doi:10.1113/jphysiol.2003.053371.

Li DP, Chen SR, Pan HL. Nitric oxide inhibits spinally projecting paraventricular neurons through potentiation of presynaptic GABA release. *J Neurophysiol* 88: 2664–2674, 2002. doi:10.1152/jn.00540.2002.

Maggesissi RS, Gardino PF, Guimarães-Souza EM, Paes-de-Carvalho R, Silva RB, Calaza KC. Modulation of GABA release by nitric oxide in the chick retina: different effects of nitric oxide depending on the cell population. *Vision Res* 49: 2494–2502, 2009. doi:10.1016/j.visres.2009.08.004.

Merino JJ, Arce C, Naddaf A, Bellver-Landete V, Oset-Gasque MJ, González MP. The nitric oxide donor SNAP-induced amino acid neurotransmitter release in cortical neurons. Effects of blockers of voltage-dependent sodium and calcium channels. *PLoS One* 9: e90703, 2014. doi:10.1371/journal.pone.0090703.

Merritt JE, Armstrong WP, Benham CD, Hallam TJ, Jacob R, Jaxa-Chamiec A, Leigh BK, McCarthy SA, Moores KE, Rink TJ. SK&F 96365, a novel inhibitor of receptor-mediated calcium entry. *Biochem J* 271: 515–522, 1990. doi:10.1042/bj2710515.

Mills SL, Massey SC. Differential properties of two gap junctional pathways made by AII amacrine cells. *Nature* 377: 734–737, 1995. doi:10.1038/377734a0.

Miyachi E, Murakami M, Nakaki T. Arginine blocks gap junctions between retinal horizontal cells. *Neuroreport* 1: 107–110, 1990. doi:10.1097/00001756-199010000-00006.

Pan L, Wu X, Zhao D, Hessari NM, Lee I, Zhang X, Xu J. Sulfhydryl modification induces calcium entry through IP_3-sensitive store-operated pathway in activation-dependent human neutrophils. *PLoS One* 6: e25262, 2011. doi:10.1371/journal.pone.0025262.

Pang JJ, Gao F, Wu SM. Light responses and morphology of bNOS-immunoreactive neurons in the mouse retina. *J Comp Neurol* 518: 2456–2474, 2010. doi:10.1002/cne.22347.

Peters JM, Walsh MJ, Franke WW. An abundant and ubiquitous homo-oligomeric ring-shaped ATPase particle related to the putative vesicle fusion proteins Sec18p and NSF. *EMBO J* 9: 1757–1767, 1990.

Prakriya M, Lewis RS. Potentiation and inhibition of Ca(2+) release-activated Ca(2+) channels by 2-aminoethyldiphenyl borate (2-APB) occurs independently of IP(3) receptors. *J Physiol* 536: 3–19, 2001. doi:10.1111/j.1469-7793.2001.t01-1-00003.x.

Reid CA, Bekkers JM, Clements JD. Presynaptic Ca^{2+} channels: a functional patchwork. *Trends Neurosci* 26: 683–687, 2003. doi:10.1016/j.tins.2003.10.003.

Richter JM, Schaefer M, Hill K. Clemizole hydrochloride is a novel and potent inhibitor of transient receptor potential channel TRPC5. *Mol Pharmacol* 86: 514–521, 2014. doi:10.1124/mol.114.093229.

Rothman JE. The protein machinery of vesicle budding and fusion. *Protein Sci* 5: 185–194, 1996. doi:10.1002/pro.5560050201.

Singh A, Hildebrand ME, Garcia E, Snutch TP. The transient receptor potential channel antagonist SKF96365 is a potent blocker of low-voltage-activated T-type calcium channels. *Br J Pharmacol* 160: 1464–1475, 2010. doi:10.1111/j.1476-5381.2010.00786.x.

Smith SM, Chen W, Vyleta NP, Williams C, Lee CH, Phillips C, Andresen MC. Calcium regulation of spontaneous and asynchronous neurotransmitter release. *Cell Calcium* 52: 226–233, 2012. doi:10.1016/j.ceca.2012.06.001.

Tarasenko A, Krupko O, Himmelreich N. New insights into molecular mechanism(s) underlying the presynaptic action of nitric oxide on GABA release. *Biochim Biophys Acta* 1840: 1923–1932, 2014. doi:10.1016/j.bbagen.2014.01.030.

Tekmen-Clark M, Gleason E. Nitric oxide production and the expression of two nitric oxide synthases in the avian retina. *Vis Neurosci* 30: 91–103, 2013. doi:10.1017/S0952523813000126.

Tooker RE, Vigh J. Light-evoked *S*-nitrosylation in the retina. *J Comp Neurol* 523: 2082–2110, 2015. doi:10.1002/cne.23780.

Tozer AJ, Forsythe ID, Steinert JR. Nitric oxide signalling augments neuronal voltage-gated L-type (Ca(v)1) and P/q-type (Ca(v)2.1) channels in the mouse medial nucleus of the trapezoid body. *PLoS One* 7: e32256, 2012. doi:10.1371/journal.pone.0032256.

Tsukamoto Y, Morigiwa K, Ueda M, Sterling P. Microcircuits for night vision in mouse retina. *J Neurosci* 21: 8616–8623, 2001.

Usmani SM, Fois G, Albrecht S, von Aulock S, Dietl P, Wittekindt OH. 2-APB and capsazepine-induced Ca^{2+} influx stimulates clathrin-dependent endocytosis in alveolar epithelial cells. *Cell Physiol Biochem* 25: 91–102, 2010. doi:10.1159/000272064.

Vigh J, Lasater EM. L-type calcium channels mediate transmitter release in isolated, wide-field retinal amacrine cells. *Vis Neurosci* 21: 129–134, 2004. doi:10.1017/S095252380404204X.

Wall MJ. Endogenous nitric oxide modulates GABAergic transmission to granule cells in adult rat cerebellum. *Eur J Neurosci* 18: 869–878, 2003. doi:10.1046/j.1460-9568.2003.02822.x.

Wang GY, Liets LC, Chalupa LM. Nitric oxide differentially modulates ON and OFF responses of retinal ganglion cells. *J Neurophysiol* 90: 1304–1313, 2003. doi:10.1152/jn.00243.2003.

Wang JP. GEA3162 stimulates Ca^{2+} entry in neutrophils. *Eur J Pharmacol* 458: 243–249, 2003. doi:10.1016/S0014-2999(02)02790-5.

Warrier A, Borges S, Dalcino D, Walters C, Wilson M. Calcium from internal stores triggers GABA release from retinal amacrine cells. *J Neurophysiol* 94: 4196–4208, 2005. doi:10.1152/jn.00604.2005.

Watanabe S, Koizumi A, Yamada Y, Kaneko A. Functional roles of action potentials and na currents in amacrine cells. In: *The Neural Basis of Early Vision*, edited by Kaneko A. Tokyo: Springer-Verlag, 2003, vol. 11, p. 55–58.

Xing J, Li DP, Li J. Role of GABA receptors in nitric oxide inhibition of dorsolateral periaqueductal gray neurons. *Neuropharmacology* 54: 734–744, 2008. doi:10.1016/j.neuropharm.2007.12.008.

Yang S, Cox CL. Modulation of inhibitory activity by nitric oxide in the thalamus. *J Neurophysiol* 97: 3386–3395, 2007. doi:10.1152/jn.01270.2006.

Yoshida T, Inoue R, Morii T, Takahashi N, Yamamoto S, Hara Y, Tominaga M, Shimizu S, Sato Y, Mori Y. Nitric oxide activates TRP channels by cysteine S-nitrosylation. *Nat Chem Biol* 2: 596–607, 2006. doi:10.1038/nchembio821.

Yu D, Eldred WD. Nitric oxide stimulates gamma-aminobutyric acid release and inhibits glycine release in retina. *J Comp Neurol* 483: 278–291, 2005. doi:10.1002/cne.20416.